FEDERAL UNIVERSITY OF SANTA CATARINA
DEPARTMENT OF MECHANICAL ENGINEERING
UNDERGRADUATE COURSE OF MATERIALS ENGINEERING

Diploma Thesis from

ALÍCIA CORRÊA LUCENA

Developed at University of Bremen,

ADVANCED CERAMICS GROUP

THIN FILM FORMATION OF MIXED DIFFERENT-SIZED-SILICA NANOPARTICLE/STEARIC ACID SURFACTANT AT THE WATER-OIL INTERFACE

Scientific advisors:

M.Sc. Joeri Smits

PD. Dr. rer. nat. Michael Maas

Prof. Dr.-Ing. Kurosch Rezwan

BREMEN

2020

FEDERAL UNIVERSITY OF SANTA CATARINA
DEPARTMENT OF MECHANICAL ENGINEERING
UNDERGRADUATE COURSE OF MATERIALS ENGINEERING

ALÍCIA CORRÊA LUCENA

THIN FILM FORMATION OF MIXED DIFFERENT-SIZED-SILICA NANOPARTICLE/STEARIC ACID SURFACTANT AT THE WATER-OIL INTERFACE

Thesis presented to the Materials engineering graduation course from the Federal University of Santa Catarina as partial requirement to acquire the degree of “Engenheira de Materiais”.

Supervisor: PD Dr. rer. Nat. Michael Maas

Bremen
2020

ACKNOWLEDGEMENTS

First of all, I would like to thank the Advanced Ceramics Group, headed by Prof. Dr.-Ing Kurosch Rezwan, and my supervisor PD Dr. rer. nat. Michael Maas for giving me the opportunity to work on this group and on the given project.

I would also like to thank M.Sc. Joeri Smits, for all the orientation given throughout this period and the shared knowledge, as well for the good times experienced during my time in the laboratory. I also thank all members of Advanced Ceramics Group, for the instructions and for always being friendly and cooperative.

Thanks to the internship coordinator of the undergraduate course of Materials Engineering at UFSC, in particular, the coordinator of internships Prof. Fábio Antonio Xavier, the supervisor of interns Marcus Barnetche and his assistants for providing all the necessary assistance to carry a successful internship.

A special thanks to all my dear friends in Bremen for making this time here memorable, to my friends in Brazil, for always supporting me even with distance and to my boyfriend, Arthur C. Cruzeiro, for all the enjoyable memories during this period and for the support during hard times.

I would like to thank all my family, in special my siblings and my grandparents for believing, loving and supporting me and, finally, my parents, Sirley E. Corrêa and Mauricio H. A. Lucena, for always sacrificing for me and doing everything they could to provide me the best education and opportunities.

ABSTRACT

This work aims to achieve a structure reinforcement on an interfacial film, by improving its density when adjusting smaller particles between the hexagonal interstitial spaces between the bigger ones. The packing of a two-sizes mixed silica nanoparticles film, in a water-oil interface, in a system with surfactants equally charged as the particles, was investigated. Therefore, systems of 1 w% silica nanoparticles on water phase + 1mM stearic acid surfactants on oil phase were studied, as well as reference systems without particles and/or surfactants. A formation of a viscous film was observed in interfacial shear rheology and pendant drop dilatational rheology for the systems at the pH of 9.8, in which the surfactants are deprotonated and, therefore, more surface active. The films showed a predominantly viscous behavior and the system for the smaller particles showed higher modulus when compared to the bigger ones. Scanning electron microscopy (SEM) analysis of Langmuir-Blodgett-type transfer films showed for the systems with mixed particles a less ordered system, with numerous discontinuities, when compared to the systems with only one size particles. A more quantitative analysis was performed by interfacial shear and dilatational rheology. The lower density film observed in the SEM images for the binary systems was verified by lower moduli. The self-assembly technique used for the system studied proved not to be the best approach to reach the goal of assembling a highly ordered structure.

RESUMO

O presente trabalho tem como objetivo alcançar um reforço estrutural em um filme interfacial, através do aumento da sua densidade ao ajustar partículas menores entre os espaços intersticiais hexagonais entre partículas maiores. O empacotamento de um filme com dois diferentes tamanhos de nanopartículas de sílica, misturados em uma interface de água-óleo, em um sistema com surfactantes igualmente carregados como as partículas, foi investigado. Portanto, sistemas de nanopartículas de sílica a 1% em peso na fase aquosa + 1 mM de ácido esteárico como surfactantes na fase oleosa, bem como sistemas de referência sem partículas e / ou surfactantes, foram estudados. A formação de um filme viscoso para os sistemas com pH de 9.8 foi observada nos resultados de reologia de cisalhamento interfacial e nos de reologia dilatacional de gota pendente. Nesse pH, os surfactantes estão desprotonados e, portanto, seu potencial tensoativo na superfície é reforçado. As partículas menores apresentaram valores de módulo de perda maiores e, portanto, um filme mais estruturado. A análise de Microscopia eletrônica de varredura (MEV) de filmes obtidos por transferência do tipo Langmuir-Blodgett mostrou um empacotamento com menor ordem para os sistemas com partículas mistas e com inúmeras descontinuidades quando comparado aos sistemas com apenas um tamanho de partícula. Uma análise mais quantitativa foi realizada por cisalhamento interfacial e reologia dilatacional, a densidade menor para as amostras com partículas misturadas, observado nas imagens de MEV foi verificado pelo modulo menor alcançado por esses sistemas. A técnica de automontagem utilizada para o sistema estudado mostra não ser a melhor abordagem para atingir o objetivo de montar estruturas altamente ordenadas com partículas mistas de 25 nm e 80 nm, uma vez que é possível perceber que seu empacotamento e montagem mudou ao longo do filme.

LIST OF FIGURES

TABLE OF CONTENTS

1. INTRODUCTION

Conventional emulsions are well known to be stabilized by surfactants. The interfacial tension of the interface between two immiscible liquids is reduced when the molecules adsorb there, preventing coalescence and flocculation of droplets via steric and/or electrostatic repulsion. However, these emulsions are thermodynamically unstable (XU et al., 2018). A Ramsden-Pickering emulsion, on the other hand, is an emulsion which retains the basic properties of an ordinary emulsion stabilized by surfactants, differing in the fact that it is stabilized by solid or soft materials, like colloidal particles or polymers, which replace the surfactants at the interface, providing the emulsion with a high stability, due to the fact that the particles have a high energy of attachment at the interface (BINKS; LUMSDON, 2001; CHEVALIER; BOLZINGER, 2013; TSABET; FRADETTE, 2015).

In that context, what would happen when surfactants and particles are used simultaneously in an emulsion system? Untreated oxide nanoparticles negatively charged such as silica cannot adsorb at the interface, due to the electrostatic repulsion between them and the negatively charged interface, like oil/water or air/water. Although these type of materials are not active at the liquid interface, the presence of surfactant in a system containing hydrophilic nanoparticles can strongly affect the interfacial activity of the particles, making it surface active, creating, therefore, a Pickering emulsion (CALZOLARI et al., 2012; SMITS et al., 2019; XU et al., 2018).

The investigation of colloidal nanoparticles adsorbed at fluid interfaces have attracted much attention research-wise, hence the range of applications of such particles is very wide. The self-assembly of nanoparticles at fluid-fluid interface has provided the fabrication of high-quality two dimensional crystals, due to the fact that, by forming ordered structures on macroscopic scales, it combines the advantages of having the nanoscale properties with large-scale structures. (BRESME; OETTEL, 2007; MAAS; OOI; FULLER, 2010). Most researches focus on the fabrication of colloidal crystals with single diameter colloidal spheres. However, recent studies have shown many advantages on using colloidal spheres of two sizes to produce colloidal crystals, forming binary colloidal crystals (bCCs), when compared to colloidal crystals with single size-sized colloidal spheres (DAI et al., 2012).

Aiming the characterization of interfaces existing in big interface area systems like emulsions, foams and thin films, Interfacial rheology can be used. The property of surface tension is usually sufficient to characterize a simple interface, however more complex ones can

be formed when surface active species, like particles, are present, forming a highly structured fluid-fluid system that can lead to an interfacial viscoelastic response. That being said, the interfacial properties can no longer be defined by surface tension alone, leading to the necessity to investigate interfacial rheology (RENGGLI et al., 2020).

In this study a system of silica nanoparticles and surfactants equally charged interacting on a water-oil interface is studied. This work aims the reinforcement of the created film by mixing two different sized particles, in order to improve the packing of the nanoparticles at the interface. The theory behind it is that by self-assembly technique of particles in a system with surfactants equally charged, the particles would be able to rearrange better in the interface, since they are not trapped there, due to the fact that the particles and the surfactants are equally charged, creating an adsorption/desorption mechanism in the system, providing a reversible nature for the particles adsorption. Therefore, for a system where two different sizes of nanoparticles are mixed together, the smaller ones could rearrange on the hexagonal interstitial spaces between the bigger ones, as these last ones arrive first at the interface, optimizing the packing and, consequently, forming a fortified particle monolayer that will enhance rheological properties, such as higher Moduli.

In order to evaluate the hypothesis, aqueous silica nanoparticles solutions were used as the dispersion environment, silica powder for the 80 nm and silica Ludox for the 25 nm at pH of 6 and 9.8. The oil phase was composed by a 1mM stearic acid dispersion on decane. In order to characterize the system studied, interfacial rheology measurements were performed by a rotational shear rheometer (DHR), using a thin Du Noüy ring placed at the interface and shear in oscillating manner, as well as Pendant Drop Dilatational Interfacial Rheology. Furthermore, scanning electron microscopy (SEM) images of the monolayer structure formed and dynamic light scattering (DLS) measurements of the particle solutions were carried in order to help characterizing the system and the rheological measurements.

2. LITERATURE REVIEW

2.1. SILICA NANOPARTICLES

2.1.1. Nanomaterials

Nanomaterials are functional materials characterized by being particulates with at least one-dimension bellow 100 nanometers (nm) and having significantly different properties from its bulk material. Therefore, nanomaterials possess incredible electronic, thermal, mechanical and biological properties that can't be found in conventional materials, which leads them to have extensive applications in Physical, Chemical and Biological Sciences, at the Engineering field and Computer Science (HAMZA; IORHEMEN; TAY, 2016). Among the types of nanomaterials, nanoparticles are the most well-known. These type of materials have a high reactivity as a consequence of their surface effects, since there is a high quantity of atoms located on its surface, subjecting them to phase transformation (MISHRA et al., 2018).

2.1.2. Silica

In the present study, amorphous nanoparticles of silicon dioxide are employed, in different sizes and generally negatively charged. Silicon dioxide (SiO_2), an inorganic ceramic material also known as silica, is the most abundant material on earth. Silica atoms are non-metal oxides and are composed of one silicon atom surrounded by four oxygen atoms in a tetrahedral geometry. The very directional and strong covalent bonding present in the molecule results in a very hard material. It can be found in nature or produced synthetically, occurring in a wide range of structures, from totally amorphous forms to highly crystalline ones, such as quartz (YADAV; RAIZADAY, 2016).

Due to the flexibility of bridging between the atoms in the silica molecule, this material possesses the possibility to varies its structural arrangement (YADAV; RAIZADAY, 2016). Silica presents itself in tetrahedral unities SiO_4 distributed randomly and united by siloxane bridges, Si-O-Si, in its interior. It also contains vicinal

silanols, Si-OH, and germinal silanols, HO-Si-OH, dispersed in the surface, those which are sensitive to reactions that enable the chemical modifications of its matrix (PRADO; FARIA; PADILHA, 2005).

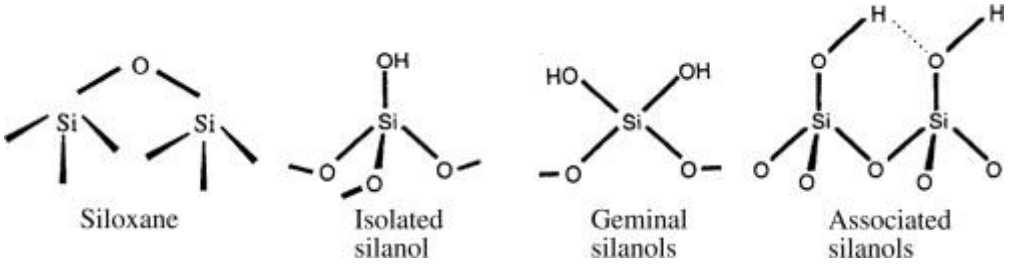

Figure 1: Types of silanol groups. (POOLE, 2015)

2.2. SURFACTANTS

Surfactants are substances which create self-assembled molecular clusters, called micelles, in a solution (water or oil phase) and adsorb to the interface between a solution and a different phase. What allows the surfactant to have these two physical properties is its chemical structure that contains two different functional groups with dissimilar affinity within the same molecule (NAKAMA, 2017).

The hydrophobic group, which does not show affinity to water, is usually an alkyl chain with 8 to 22 carbons. When used in lipid system, they can be called lipophilic. The hydrophilic part of the surfactant is the one that has affinity with water. This structure were two opposing groups with opposing functions are present is called amphiphilic structure. Surfactants can be classified according to its ionization (ionic and nonionic) and also depending on their solubility, either if they are soluble in water or lipids. Ionic surfactants usually are hydrophilic as well, but the nonionic ones can be hydrophilic or lipophilic, depending on the balance of the hydrophilic and lipophilic groups (NAKAMA, 2017).

The surfactant used in this study is the Stearic Acid (Figure 2). This material is a saturated fatty acid made of an 18-carbon chain and its IUPAC name is octadecanoic acid. Therefore, it has a polar had group and a nonpolar chain, providing it the amphiphilic characteristic.

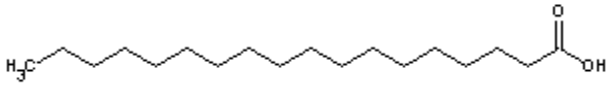

Figure 2: Stearic Acid molecule. Available at -https://www.chemsynthesis.com/base/chemical-structure-24602.html-.

2.3. RAMSDEN-PICKERING EMULSION

Conventional emulsions are well known to be stabilized by surfactants. The interfacial tension of the interface between two immiscible liquids is reduced when the molecules adsorb there, preventing coalescence and flocculation of droplets via steric and/or electrostatic repulsion, however, these emulsions are thermodynamically unstable (XU et al., 2018).

A Ramsden-Pickering emulsion, on the other hand, is an emulsion which retains the basic properties of an ordinary emulsion stabilized by surfactants, differing in the fact that it is stabilized by solid or soft materials (for example, colloidal silica or polymers), which adsorb onto the interface of two immiscible phases, instead of surfactants. This surfactant-free characteristic makes it appealing to several application, especially for cosmetic and pharmaceutical industries, since surfactant can often show adverse effects (CHEVALIER; BOLZINGER, 2013). The Figure 3 bellow shows an illustration of both emulsions.

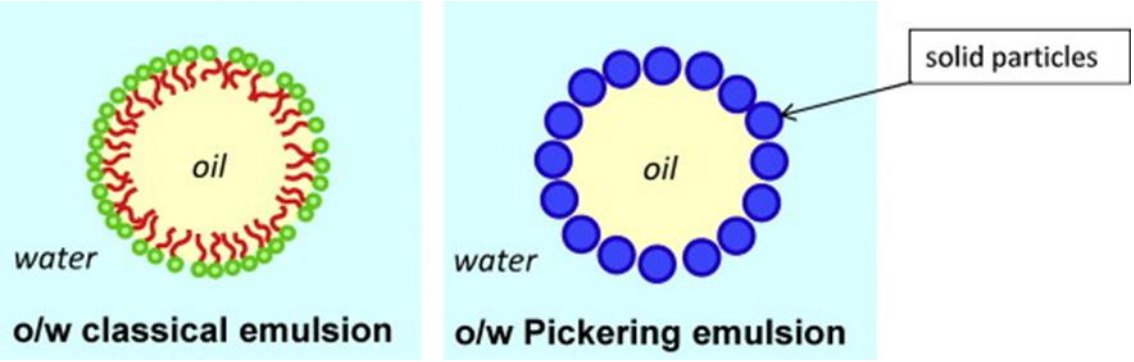

Figure 3: illustration of both classical emulsion stabilized by surfactants and a Pickering emulsion stabilized by particles. (Chevalier & Bolzinger, 2013)

Such emulsions have specific properties due to its stabilization by a solid particle, particularly the high resistance to coalescence, which is accomplished by the high energy of attachment for particles at the liquid-liquid interface, which gives the emulsion a high stability. It is shown that particles have more potential to produce highly stable emulsions when compared to surfactants. These solid particles are necessarily smaller than the emulsion droplets, therefore, particles in the nanometric scale allow stabilization of a few micrometer droplets (BINKS; LUMSDON, 2001; CHEVALIER; BOLZINGER, 2013; TSABET; FRADETTE, 2015).

It was also shown that is possible to increase even more the stability of emulsions by having a close-pack lattice formed by the particles, due to capillary force and particle interactions at the interface. Therefore, in order to analyze the stability of the emulsion, the

interface must be taken into consideration. In that context, studies have shown that when highly hydrophobic or hydrophilic particles are used, the emulsion is less stable, so intermediate wettability would lead to a higher stability. What can also increase the stability is higher particle concentrations, smaller particle sizes or the use of monodispersed particles (TSABET; FRADETTE, 2015; YAN et al., 2015).

2.4. FORMATION OF MONOLAYER FILM

2.4.1. Formation of 2D binary colloidal crystals

Colloidal crystals with a two-dimensional (2D) or three-dimensional (3D) arrangement of monodispersed colloidal spheres have been catching attention research-wise, mostly on the fabrication of colloidal crystals with a single diameter colloidal spheres. However, recent studies have shown many advantages on using colloidal spheres of two sizes to produce colloidal crystals, forming binary colloidal crystals (bCCs), when compared to colloidal crystals with single sized colloidal spheres (DAI et al., 2012). These type of crystals were first observed in Brazilian opals.

BISHOP et al., (2009) shows in his study that self-assembled monolayers driven by Van der Waal forces results in the formation of a hexagonal closed-pack structure with a size-selective sorting effect. This effect happens due to the fact that the overall potential energy of the system is minimized when the bigger particles are in the center of the structure and the smaller ones will occupy the borders of the larger particles. This can also be explained with the work of OHARA et al., (1995), where is shown that in a system containing more than one size colloidal particles, the bigger ones show a greater interaction between each other when compared to the smaller ones, despite that considering the overall forces for a defined area will be greater for the smaller ones.

DAI et al., (2012) introduced a diagram as a guideline to form monolayer bCCs with different structures or patterns. They show that the number ratio of large to small spheres in a monolayer correspond to stoichiometry and specific patterns/structures of the bCC. That being said, they developed a phase diagram using the following equation (Equation 1) as a way to effective design the desired pattern of monolayer bCCs and determine their structures from the used volume and size ratios of small and large silica particles.

$$N_{S/L} = \frac{V_{S/L}}{(\phi_{S/L})^3} \quad (1)$$

Where $N_{S/L}$ is the number ratio of small to large particles, $V_{S/L}$ is the volume ratio of small and large particles and $\Phi_{S/L}$ is the size ratio of small and large particles. In order to obtain a stable monolayer bCCs, DAI et al., (2012) defined that the size ratio of the small to large particles should be in the range of $0.077 \leq \Phi_{S/L} \leq 0.577$. This work uses this definition to calculate the proper number ratio for the different-size silica particle solutions.

2.4.2. Internal and external forces involved

Self-assembly of colloidal particles is a complex process involving the balance of internal (attractive and repulsive) and external forces directing crystal growth into a stable structure and forming 2D/3D complex structures, being the statutory way for producing bCCs. The final structure, or the packing state, is related to the volume fraction and size ratios of the large and small particles. The packing of a film tends to arrange in the lowest free energy of the system. For particles of only one size, this results in hexagonal packing, with interstitial spaces between the particles (DAI et al., 2012; DIBA et al., 2018).

Basically, self-assembly of colloidal nanoparticles is governed by the balance of the following forces: Electrostatic, Van der Waal, Capillary, Depletion, Gravitational and Electro-magnetic. Figure 4, presented by DIBA et al., (2018), shows a summary of these forces.

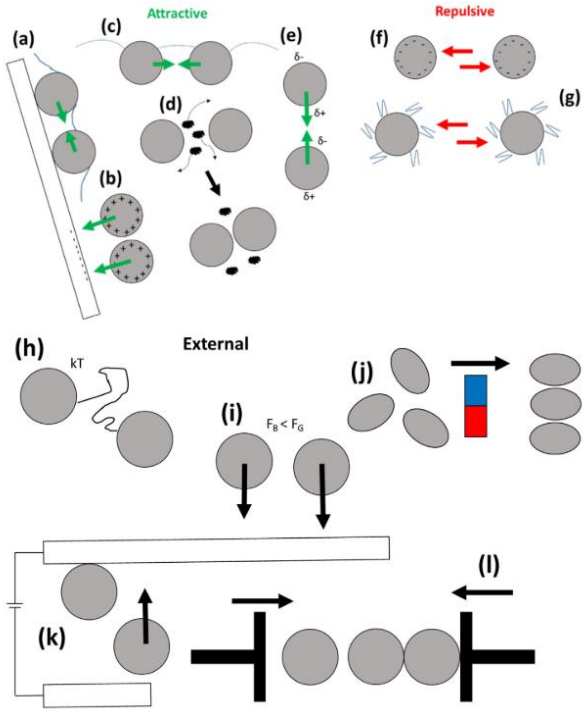

Figure 4: "Summary of the various interactions and forces encountered during colloidal self-assembly. Attractive forces; (a)immersion capillary forces, (b)electrostatic attraction, (c)flotation capillary forces, (d)depletion forces, (e)van der Waals forces. Repulsive forces; (f)electrostatic repulsion, (g)steric repulsion. External forces; (h)Brownian motion, (i)gravitational forces, (j)magnetic field, (k)electric field, and (l)forced convection" (DIBA et al., 2018).

Lateral capillary forces occur due to the liquid surface deformation, caused by particles, when it should be flat in the absence of those. This phenomenon happens in a way that the capillary interaction between these particles increases with the increase of the interfacial deformation. With the deformation of the meniscus at the liquid surface, the gravitational potential energy of the particles decreases as they approach another one, causing an attraction between them at the interface. In that context, the particle weight is the origin of the force. This force also appears in particles partially immersed in a liquid layer on a substrate, but in that case, the deformation is due to the wetting properties of the particle surface and the contact angle (KRALCHEVSKY et al., 1994; PAUNOV et al., 1993; CHAN et al., 1981; NICOLSON et al., 1949).

The electrostatic forces involved in this process can be explained by the attractive and repulsive forces present in the particle surfaces, due to their protonated and de-protonated functional groups. However, the most crucial force on the formation of ordered colloidal crystals is the repulsive one, when in the absence of it, the monolayers tend to be disordered (LI; JOSEPHSON; STEIN, 2011). The control of the surface charge can be problematic with binary suspensions, since the large and small particles have different degrees of ionic shielding and hydration. Following the

equilibrium, oppositely charged particles will attract each other and aggregate unless something else stabilizes them, like the addition of surfactants, salts or changes at the pH, for example, that will increase the repulsive electrostatic forces between the particles and, therefore, make less strong the attractive capillary forces. These techniques will give the particles more time to stabilize at a more energetically favorable position (DIBA et al., 2018; OH et al., 2011; VOGEL et al., 2011; WANG et al., 2015).

Van der Waals forces appear in the cases where the colloidal particles overcome the repulsive electrostatic forces, getting closer to one another, since is a universal force present on surface interactions. These forces bring the particles together forming a long-range assembly and depend on the size and shape of the colloidal particles, their magnitude can be considered much greater than the thermal energy (kT) of the particles. (BARTLETT; CAMPBELL, 2005; BRÜGGER et al., 2015; DIBA et al., 2018).

In the formation of bCCs structures, attractive depletion forces take place influencing the aggregation of the colloidal particles. In binary systems with small and large particles, for the smaller ones to occupy the space between the bigger ones, their size should be smaller than the distance between one large particle to another. If that does not occur, the smaller particles are expelled from the volume around the large particles (DIBA et al., 2018; SINGH et al., 2011).

2.4.3. Self-assembly technique of nanoparticles at fluid-fluid interface

Self-assembly is a process in which ordered superstructures are formed by the spontaneously arrange of nanomaterials. The self-assembly of nanoparticles at fluid-fluid interface has provided the fabrication of high-quality two dimensional colloidal crystals. By forming ordered structures on macroscopic scales, the advantages of having the nanoscale properties with large-scale structures are combined. In that context, nanoparticles have been used as building blocks for materials with specific properties and it is of interest to investigate new ways for the preparation of self-assembled and durable nanostructured materials, such as cohesive films. (BRESME; OETTEL, 2007; LI; JOSEPHSON; STEIN, 2011; MAAS; OOI; FULLER, 2010).

Following the theory proposed by DAI et al., (2012), the density of a film made of particles could be improved by adjusting smaller particles in the gaps between the

bigger particles, increasing the order by lowering the free spaces and energy, generating, therefore, a structure reinforcement.

Langmuir trough techniques facilitates the transfer of the crystal monolayers to a solid interface, by providing a mean to tune the interparticle distances. Nanoparticles are more sensitive to thermal fluctuations when compared to bigger scales like micro and they show stronger dependence with interfacial forces, what leads to a particle size dependent self-assembly (BRESME; OETTEL, 2007; FENDLER, 1996).

Capillary forces tend to influence the self-assembly of nanoparticles at the interface, when it comes to macroscopic particles, the deformation occurs due to the particle's weight, however, for the nanoscale gravity do not have the same influence. Nonetheless, some forces play a role at the nanoscale, like immersion forces and electric field induced capillary interactions of charged particles. The interactions between particles at the interface cannot be as easily explained as for the bulk, since there are other factors to be considered like the deformability of the interface and its inherent discontinuities. Particle adsorption at a fluid-fluid interface significantly reduces the interfacial area between the two, decreasing the interfacial free energy and, thereby, in models of surfactants and particles differently charged, it traps the particles and form a system that is thought to be virtually irreversible. These systems provide emulsions to stabilize at very low particle concentrations (BRESME; OETTEL, 2007; KRALCHEVSKY; NAGAYAMA, 2000; LIN et al., 2003; SMITS et al., 2019).

However, when analyzing systems where the particles and the surfactants are equally charged, the behavior of the particles at the interface will be different, since then, the two species will compete for a place at the interface. SMITS et al., (2019) developed a mechanism (Figure 5) to analyze the competition between hydrophilic nanoparticles and surfactants for interfacial adsorption by studying surfactants (ODA) and particles (APTES-coated silica particles) equally positively charged diluted in immiscible liquids, restricting their interaction to the interface. The mechanism consists in a dynamic adsorption/desorption process caused by the competitive adsorption behavior in a multicomponent system, where the interaction between the two components is weak. According to SMITS et al., (2019), "A dynamic equilibrium is accomplished where the particle desorption presents a lower free-energy change, caused by the phenomenon in which the increase in interfacial area during their desorption if counteracted by simultaneous adsorption of new lipids. Due to the small activation

energy barrier of adsorption/desorption, reabsorption to a surfactant-covered interface is also possible".

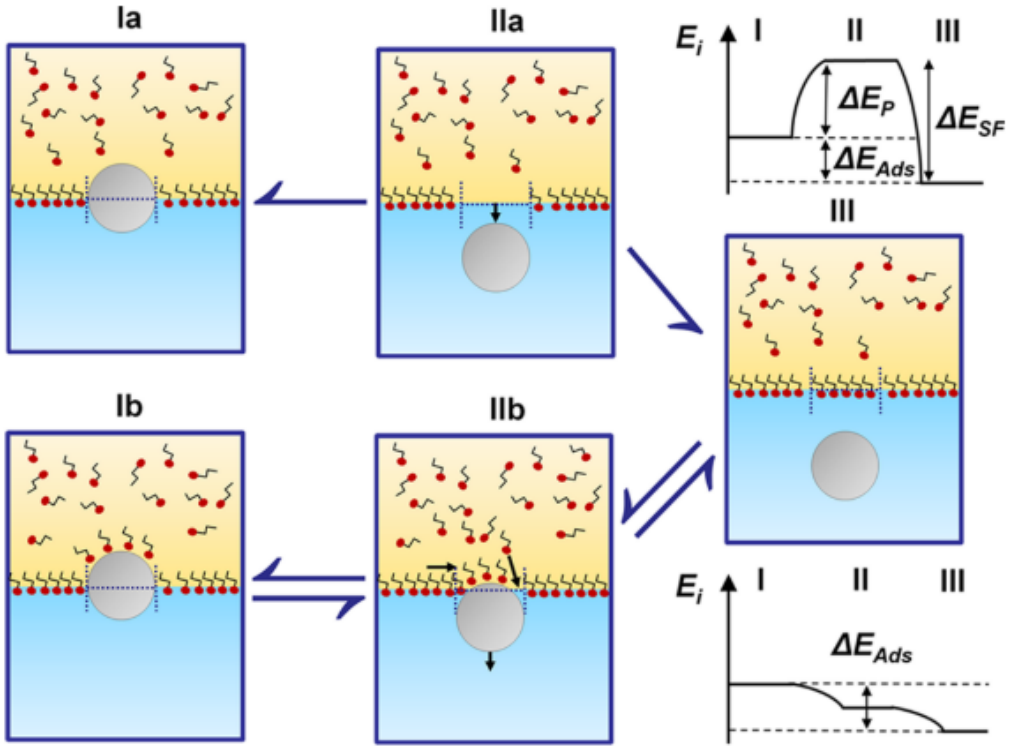

Figure 5: "Proposed competitive adsorption behavior between surfactants and nanoparticles with similarly charged groups at the decane−water interface. In the usual model (top row), particles are irreversibly trapped due to high binding energies and transition from stage Ia to stage IIa is not possible. Instead, in the presence of weakly interacting surfactants and particles, desorption of particles from the interface towards the bulk (lower row) is caused by competitive adsorption in a concentration-dependent manner with a transitional state that drastically lowers the energy barrier for particle desorption (stage IIb,). As a result, dynamic adsorption and desorption of both species exists at equilibrium, which is expressed in the energy diagrams with the interfacial free energy (Ei), the change of interfacial energy by one adsorbed nanoparticle (ΔEP), and the energy change caused by surfactant molecules covering the same area as the particles (ΔESF) and (ΔEAds = ΔESF − ΔEP)." (SMITS et al., 2019)

2.4.4. Influence of surfactants on the behavior of silica nanoparticles at the interface

Untreated oxide nanoparticles such as silica in their majority are hydrophilic and, hence, cannot adsorb to fluid-fluid interface such as oil/water or air/water. Although these type of materials are not active at the liquid interface, the presence of surfactant in a system containing silica nanoparticles can strongly affect the interfacial properties of the liquid, making it surface active. The influence at the interface of both particles and surfactants combined is still not well understood, however is known that surfactants reduce the interfacial tension, preventing flocculation and coalescence in emulsions. The study of this combination on the stabilization of emulsions can be simplified by

studying adsorption phenomena of two-dimensional immiscible interfaces (CALZOLARI et al., 2012; SMITS et al., 2019).

Combining surfactants and particles in the same bulk phase allows high adsorption of particles at the interface, nonetheless, dissolving them in different immiscible liquids focus and limits their interaction to the interface between the liquids. The silica nanoparticles when adsorbing surfactants at their surface are transformed from hydrophilic to partially hydrophobic, becoming surface-active. This partial wettability is responsible to drive the nanoparticles to the interface, forming and stabilizing emulsions. DU et al., (2010) showed that, for nanoparticles without surfactants, no interactions occur between interfacial adsorbed particles until a close-packed layer is formed, however, in a densely populated interface, the particles begin to experience different forces such as van der Waals and short-range capillary interactions (DU et al., 2010; SMITS et al., 2019).

MAAS; OOI; FULLER, (2010) studied the thin film formation of silica nanoparticle and two lipids, Stearic Acid and Stearyl Amine, at the fluid-fluid interface. They studied Ludox silica nanoparticles, which have negative surface charges and form stable dispersions in water, combined it with an equally negatively charged lipid (stearic acid) and a positively charged lipid (stearyl amine). Their work shows that interaction forces between the particles and lipids play and important role for the formation of the film, in a way that the stable dispersion of the Ludox particles can become unstable if the surface charges of the particles become shielded or neutralized. For the system with the negatively charges stearate, the same used in this work, the interaction with the particles is less strong and intuitive as for the positive ones, but still, like said before, the presence of the lipids by itself next to the interface can lead to the shielding of the negative charges of the silica particles, making their double-layer become more and more compressed until the dispersion becomes unstable due to the domination of dispersive forces. However, this approach has a complication due to the fact that the negatively charged interface possibly present a diffusion barrier to the particles (MAAS; OOI; FULLER, 2010).

2.5. RHEOLOGY

2.5.1. Fundamentals

Rheology is the term given to the science of deformation and flow. It originates from the Greek: “thein” which means “to flow”. Therefore, rheology can be explained as the flow science and is a subdivision of physics and physical chemistry, having the most relevant variables coming from the field of mechanics. Not only rheological experiments reveal information about flow behavior of liquids, but also about deformation behavior of solids, therefore, it can characterize viscoelastic materials. The connection is that a large deformation produced by shear forces causes many materials to flow (MEZGER, 2019).

All real materials have their behavior based on a combination of both viscous and elastic portion, the so called viscoelastic behavior. In this context, all types of shear comportments can be seen as staying between two extremes: on one side the flow of ideally viscous liquids and on the other one the deformation of ideally elastic solids (MEZGER, 2019).

The idealviscous behavior follows Newton’s law and can be explained by the dashpot model. The idealelastic behavior follows Hooke’s law and can be explained by the spring model. In that context, the viscoelastic materials will behave with a combination of both models. Viscoelastic liquids behave by Maxwell’s model, where the spring (elastic portion) and the dashpot (viscous portion) are joined in a serial connection (Figure 6). When applying and removing a load on these type of materials, a remaining deformation will be presence and can be explained by the fact that elastic portion (spring) will come back to its original state but the viscous portion (dashpot) will not. Viscosity is present when talking about flowing fluids, as their molecules show relative motion between each other, what results in internal friction forces and, therefore, flow resistance when put in motion. All the materials which show flow behavior are defined as fluids (MEZGER, 2019).

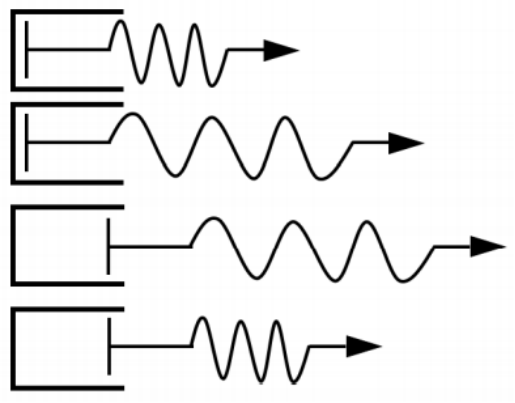

Figure 6: Maxwell model.

On the other hand, viscoelastic solids will follow Kelvin/Voigt model (Figure 7), where the spring and the dashpot are joined in a parallel connection. That being said, when applying and removing a load on these materials, they will not show residual deformation, since the elastic part (spring) will pull the viscous part (dashpot) to its original state, however, the reformation will show a delay, since the viscous part will show some resistance to go back (MEZGER, 2019).

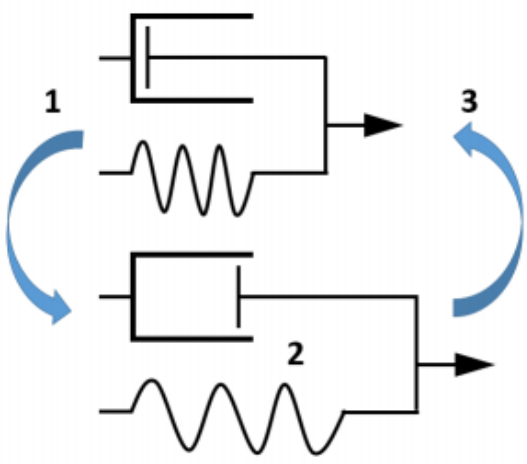

Figure 7: Kelvin/Voigt model.

The measuring technology behind obtaining rheological data from the materials is called Rheometry. This method uses rotational and oscillatory rheometers to investigate both solids and liquids. In order to characterize viscous behavior, rotational tests are performed. However, to investigate viscoelastic behavior, creep tests, relaxation tests and oscillatory tests are performed (MEZGER, 2019).

To define some of the fundamental rheological parameters, the Two-Plates-Model (Figure 8) is used. In this model, the upper plate moves while the lower plate is stationary, therefore, when a shear force (F) is applied, the upper plate moves and its resulting velocity (v) is measured. It is assumed that the liquid adheres to both plates,

not sliding along them, and also the conditions of flow are laminar. “A” is the shear area and “h” the distance between the two plates, a gap where the liquid sample will be sheared, and Φ is the deflection angle. The shear stress τ is defined by the division of the force (F) for the area (A) and the shear rate $\dot{\gamma}$ is defined by the division of the velocity (v) for the distance (h) between the plates (MEZGER, 2019).

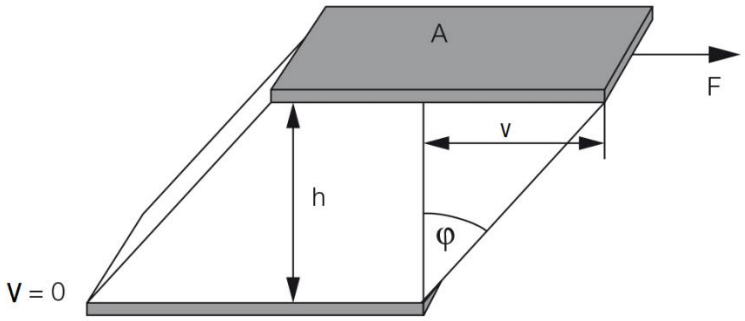

Figure 8: Two plates model. Available at -https://wiki.anton-paar.com/de-de/grundlagen-der-rheologie/-.

For oscillatoy tests in Shear Rheology, another version of the Two-Plates-Model is used. The mechanism follows the same explained before, however, as seen in Figure 9, the upper plate is connected to a wheel by a rod while the bottom plate stays stationary. As the wheel turns, the upper plate moves back and forth, as the wheel performs a full rotation angle of 360° and the resulting force is measured at the lower plate. The test corresponds to the time-dependent functions $\tau(t)$, γ(t) and $\dot{\gamma}$(t) . For the angle positions of 90° the upper plate is at its maximum deflection to the right, at 270° to the left and at the angle positions of 0° and 180° the upper plate is at zero (MEZGER, 2019).

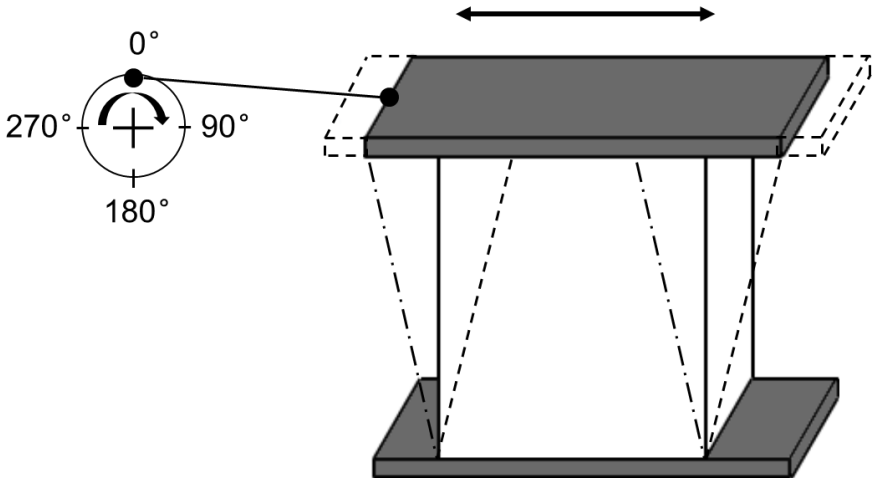

Figure 9: “Using the Two-Plates-Model for oscillatory shear test” (MEZGER, 2019).

For oscillatory tests with idealviscous materials, according to Newton, the behavior is defined by the following equation:

$$\tau(t) = \eta^* \times \dot{\gamma}(t) \quad (2)$$

and for the idealelastic behavior, according to Hooke's law, is defined by the following equation:

$$\tau(t) = G^* \times \gamma(t) \quad (3)$$

with the complex shear modulus G*, the complex viscosity η* the complex and the time-dependent values of the sine functions of τ, γ and $\dot{\gamma}(t)$ (MEZGER, 2019).

For idealelastic materials, for the positions of 270° and 90° γ = 0, τ = 0 and the velocity is at its maximum. For the positions of 0° and 180° the velocity at these points is zero and τ and y are the maximum values. Therefore, the shear strain curve and the shear stress curve will always be in phase (Equation 3), showing sine curves with simultaneous cycles and, consequently, the phase shift angle between them will be 0°. For idealviscous materials, since they have a flow resistance that can be considered as η*, following Equation 2, the shear strain function will have a delayed response when the force is applied, therefore the τ curve will be in phase with the velocity ($\dot{\gamma}$) and will be delayed in relation to the γ curve. As a conclusion, the phase shift angle between the two functions will be 90°. In that context, as Figure 10 illustrates, for oscillatory tests of idealviscous materials, the phase shift angle between the sine curve of the shear stress function and the shear strain function will be between 0° and 90° (MEZGER, 2019).

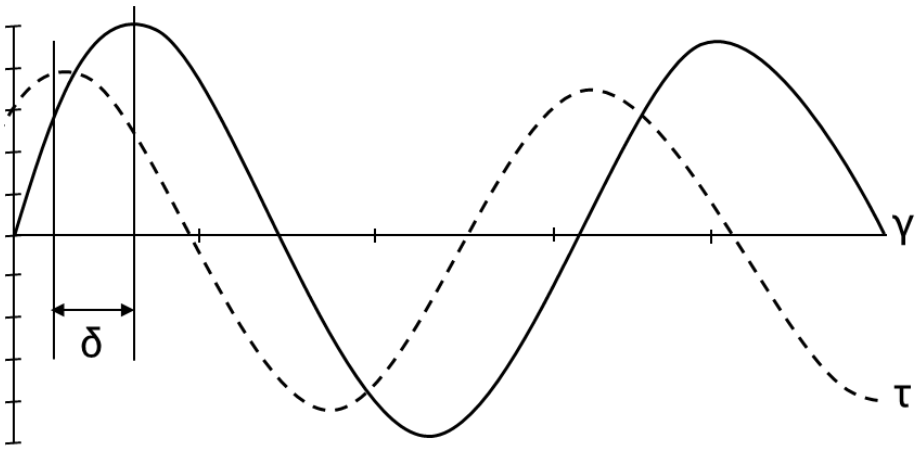

Figure 10: "Preset shear strain function γ(t), and resulting shear stress function τ(t) showing the same frequency but between the preset and the resulting sine curves occurs the phase shift angle" (MEZGER, 2019).

When performing oscillatory tests, there are some parameters used to measure and to analyze the results. Storage Modulus G', represented in Equation 4, is the result of the deformation energy stored by the sample during the shear stress, that being said,

it represents the elastic behavior of the tested material. The Loss Modulus G'', represented in Equation 5, is the result of the deformation energy used up by the sample during the shear stress and represent the viscous behavior of the tested material. The Complex Modulus G* is defined by Equation 6 and the relation between G', G'' and G* is illustrated by Equation 7:

$$G' = \left(\frac{\tau}{\gamma}\right) \times \cos \Phi \quad (4)$$

$$G'' = \left(\frac{\tau}{\gamma}\right) \times \sin \Phi \quad (5)$$

$$G^* = \tau(t)/\gamma(t) \quad (6)$$

$$|G^*| = \sqrt{(G')^2 + (G'')^2} \quad (7)$$

(MEZGER, 2019).

2.5.2. Interfacial Rheology

Interfacial rheology studies deformation and flow of thin films at a liquid/liquid or liquid/gas interface, in other words, it investigates the relationship between interfacial stress and the resultant deformation of the interface. It is a technique that is able to characterize the mechanical behavior of interfaces in big interface area systems such as emulsions, thin films and foams. Rheological properties of films at an interface can be measured by the two following methods: Interfacial shear rheology and Interfacial dilational rheology. The first one represents 2D rotational bulk shear techniques and the second, 2D bulk elongation techniques (MAAS; OOI; FULLER, 2010; MURRAY, 2002; RICHARDS, 2001).

Interfacial shear rheology measures the mechanical strength of the adsorbed layer by shearing it and promoting a change of shape of the interface. This technique can be explained as a distortion of the shape of the infinitesimally thin piece of the material, with different stresses on its edges, which translate in term of interfacial shear viscosity and elasticity (MURRAY, 2002; RICHARDS, 2001).

Interfacial dilatational rheology, on the other hand, measures the resistance to compression and expansion of the adsorbed layer, it is determinate by the change in the interfacial tension due to a specific change in the interfacial area. This type of disturbance can be correlated to pulling at the edges of an infinitesimally thin piece of material with equal stresses on all sides, so that even though the size changes, the shape

of the material is continued. In terms of viscosity and elasticity, if the material is liquid-like the first one will be defined by its resistance to flow, if the material is solid-like, the second parameter will be defined by the tensile resistance to the disturbance (MURRAY, 2002; RICHARDS, 2001).

As mentioned before, the investigation of the interface properties of Pickering emulsions can be used to study their stability, therefore, one of this technique's application is to analyze the interfacial rheology properties of these type of systems. Interfacial films have very low moduli and also low linear viscoelastic threshold values, since are such delicate system, therefore, the resulting stress values are always on the edge of the sensitivity of the rheomether (MAAS; OOI; FULLER, 2010; RENGGLI et al., 2020b). The first to suggest the concept of interfacial viscosity was Plateau, he used a magnetic compass needle on an interface to generate a shear flow. However, this technique was not the most appropriate, so alternative means of measuring the interface properties ate the magnetic microdisk, bicone and double wall ring (DWR) (RENGGLI et al., 2020b).

As this study has its focus on investigating the formation of a thin film in a liquid-liquid interface, interfacial shear rheology technique was used trough oscillatory steady-shear measurements, performed with a Du Noüy ring as the interfacial probe. Interfacial dilatational rheology technique was used trough Pendant Drop measurements.

2.5.2.1. System Inertia

RENGGLI et al., (2020) investigated the different experimental challenges and developed a generic methodology that provides a clear definition of the operating limits of various interfacial rheometers, including the interfacial needle shear rheometer, the double wall ring, and the bicone geometries.

As mentioned before, accurate measurement of interfacial rheology is still not so simple. The interfaces are very thin, therefore, the force on the rod and the torque on the ring and disks are weak when compared to the whole bulk material, making these measurements very often being operated close to the limits of the rheometer. This difficulty is also due to the fact that different devices have its own sensitivity, also that the perimeter in contact with the interface when compared to the overall surface area in contact with the bulk fluids is different for each technique, since its

used a rod, a ring and a disk. In this context, since the contribution of the interface is relatively weak, the inertia of the tool and instruments are going to influence on the measurements, as well as fluid inertia of the bulk phases in some cases. In addition to all that, complications such as imperfections and misalignment of the measurement geometries generate surface and line tension effects (RENGGLI et al., 2020). As the present work uses the double wall ring (DWR) rheometer, only the effect of the inertia contribution for this system is going to be discussed.

According to RENGGLI et al., (2020), "The torque or force resulting from the material response has to be larger than the contribution from the instrument inertia, similar to the case of bulk rheology". He then provides a simple equation where, for the DWR technique, $M_{material} > M_{inertia}$, where "$M_{material}$" represents the force resulting from the material response and "$M_{inertia}$" represents the contribution from the instrument inertia, and rewrites the material and inertia contributions applying a constitutive equation, leading to:

$$|G^*| > \frac{C_M}{C_\theta} I\omega^2 \tag{8}$$

Where G* is the complex modulus, I is the sum of the instrument and geometry inertia, ω is the driving frequency and C_M and C_Θ are conversion factors defined by the following equations:

$$C_{\theta,\mathrm{DWR}} = \frac{1}{1 - \frac{R^2_{\text{outer ring}}}{R^2_{\text{outer cup}}}} + \frac{1}{\frac{R^2_{\text{inner ring}}}{R^2_{\text{inner cup}}} - 1} \tag{9}$$

$$C_{M,\mathrm{DWR}} = \frac{1}{2\pi\left(R^2_{\text{inner ring}} + R^2_{\text{outer ring}}\right)} \tag{10}$$

(RENGGLI et al., 2020).

3. MATERIALS AND METHODS

3.1. MATERIALS

Technical grade Acetone and Ethanol Absolute were obtained from VWR Chemicals, Technical grade Ethanol 99% from Chemsolute, Citric Acid ≥99.5% from Carl Roth, millipore Type 1 water (18.2 MΩcm at 25°C) from the Synergy Water Purification system. The oil utilized in the present study was Decane (≥ 99%) from Honeywell. The nano-powder (80 nm amorphous silica) was obtained from Fiber Optic Center, the silica particles of the size of 25 nm used were a suspension in H_2O LUDOX TMA colloidal silica obtained from Aldrich chemistry. The stearic acid ≥ 98.5% from Sigma-Aldrich was the surfactants used. The cuvette utilized was the High Precision Cell provided by Hellma Analytics.

3.2. METHODS

3.2.1. Cleaning procedures

Since the systems studied are very delicate and sensitive to any contaminations, cleaning procedures were required for the appliances used.

3.2.1.1. Glassware, appliances and dishes

For the glassware, everything inside is thrown away and rinsed with ethanol. Then washed with hot tap water and cleaned with soap and a sponge, followed by a demi-water wash. After that, it is cleaned with ethanol 3 times, acetone 3 times, millipore water 3 times and once again with ethanol so it would dry faster. After that, the glassware is places somewhere clean, covered by a wipe.

For the appliances such as measuring spoons and tweezers, it is first rinsed with acetone, then ethanol, millipore water and finally dried with a clean wipe.

For the crystalizing dishes used to make the SEM samples, it is placed in a falcon tube and filled with acetone. With the dishes totally submerged in acetone, it is

sonicated for 15 min. After that, the acetone is thrown away, then the tube is filled with millipore water once, thrown away, filled again and is placed in the sonicating bath for another 15 min. The last step is to repeat the same as for the water, but with ethanol. After the last sonicating bath, the dishes are placed in a petri dish covered with clean wipes and left to dry by itself.

For the stir bars used to stir the solutions, it is placed in a falcon tube and filled with acetone. With the dishes totally submerged in acetone, it is sonicated for 15 min. After that, the acetone is thrown away, then the tube is filled with ethanol once, thrown away, filled again and is placed in the sonicating bath for another 15 min. The last step is to repeat the same as for the ethanol, but with millipore water. After the last sonicating bath, the bars are dried with a clean wipe.

3.2.1.2. Rheometer

In order to clean the Do Noüy Ring, first it is rinsed with ethanol and then with Milllipore water. After that, the ring was placed in the ultrasonic bath inside a beaker filled with 6% citric acid for 30 minutes. Then rinsed with water and placed again in the bath, but this time inside a basic solution of 1mm NaOH for 1 hour. This is necessary to get rid of all particles and surfactants that may be present still, in order to not contaminate the following measurements. After that, the ring is washed once again with millipore water and ethanol and then, with using a bunsen burner, it is rapidly heated in the blue part of the flame.

The process of cleaning the Delrin Block consists in discarding everything inside, rinsing it with ethanol until everything is gone, then washing it with hot tap water and soap. After that, it is washed with demi-water, followed by acetone rinsing 3 times and ethanol rinsing another 3 times. Then the block is filled with a solution of 6% citric acid 2 times and at the second time the block is placed in a dryer on 70°C for 20 minutes. After that, with the help of cotton buds, the inside of the block is cleaned with the citric acid yet there, then the solution is discarded away and the acid is filled in once more and discarded again. After that the block is rinsed vigorously with millipore water and, at last, it is rinsed with ethanol once more to help it dry. With the assistance of a compressed air bottle, the block is then dried.

3.2.1.3. Silica powder and solution

Since the sensibility of the measuring methods in this study is very high, is required for the silica powder and silica Ludox dispersion to go through cleaning process as well.

The powder is placed on a falcon tube, approximately 25% of the total content of the tube, and then filled with millipore water until approximately 90% of the total content of the tube. Then the solution is stirred manually until the all the powder have had contact with the water. The falcon tube is then placed in a centrifuge for 2 minutes at a velocity of 2000 rpm so the particles can deposit at the bottom of the tube, separating itself from the water again. The water is then discarded and the process is repeated another 2 times. After the last time, a clean wipe is wrapped around the top of the tube and the particles are places somewhere clean to dry by itself.

The process used to clean the Ludox silica particles is dialysis. For that Zellu trans tape 6 is used. A piece of this tape is first hydrated staying submerged in a beaker with millipore water, then, one of the sides is folded 4 times and then clipped with a clean plastic clip. With the help of a disposable glass pipet, the solution is poured inside the tape and then, the upper part is also folded 4 times and clamped. The tape with the particles solution is then placed in a 2L beaker filled with millipore water, ethanol and acetic acid in the following ratio, 4:1:0,0175. It is left to stir overnight and the next day the solution is changed to only millipore water. The process of changing the water is then repeated another 8 times, changing it twice a day. After the last time, the water is changed once again, but this time is only left for 30 minutes. The dialyzed particles solution is then poured inside a clean glass bottle and kept in the fridge.

3.2.2. Silica nano-particles dispersion preparation

The first step to prepare the nanoparticles dispersion is to calculate the required amount of particle powder or Ludox solution and water. The wanted dispersion was a 1w% solution, for both 80 nm and 25 nm particles. In order to prepare 50 mL of solution of the 80 nm silica particles, using the chemical formula $C_1*V_1=C_2*V_2$ to determinate

the right values, 49.5 g of millipore water and 0.5 g of particle powder were used. For the 25 nm silica particles, since they were not obtained in powder but in a solution of dialyzed Ludox TMA, the weight percent changes for each batch of dialysis, so the same formula mentioned before was used to determinate the amount in mL of millipore water and Ludox solution necessary to prepare the solutions, using the proper value of weight percent.

For the 80 nm particle solutions, in a precision scale, first the water was poured into the glass where the solution was going to be prepared, and, with the help of a glass disposable pipette, the exact amount of water was weighted. After that, using a disposable plastic waiting plate, the particles were weighted and then poured, carefully, into the glass. For the 25 nm, the water and the Ludox solution were added together with the help of a pipette. Afterwards, the solutions were manually stirred for about 30 seconds and then places in the ultrasonic bath for 30 minutes.

After the 30 minutes of sonicating, the pH of the dispersions was adjusted to 9.8 and then the dispersion was placed in a stirring plate for 48 hours. The pH was adjusted again after 24 hours and 48 hours of preparation. After the 48 hours, the dispersion was moved to the fridge.

At the present study, fabrication of 2D binary colloidal crystals in the fluid-fluid interface through self-assembly approach, using a mixture of colloidal spheres of 80nm and 25nm, was employed. For this approach, the structures of the monolayers are determined firstly by the size ratio of large (L) to small (S) colloidal spheres and their relative content (when different type of particle are used) (TOMMASEO et al., 2007; VELIKOV et al., 2002)

3.2.3. Surfactants solution preparation

The preparation of the surfactants solutions starts by defining the amount of stearic acid and decane necessary to prepare the desired concentration of 1mM of a 50 mL solution. In order to do that the following equation was used:

$$Grams\ of\ Stearic\ Acid = molarity \times molecular\ weight \times volume$$

$$Grams\ of\ Stearic\ Acid = 1 \times 10^{-3} \times 284.48 \times 0.05$$

$$Grams\ of\ Stearic\ Acid = 0.014224g$$

Therefore, using a precision microscale, the surfactant was weighted using a weighting paper and then placed inside the glass. With the help of the spoon used to handle it, the big clumps were smashed into smaller pieced, so that faster dissolution of the surfactants would be possible. After that, 50 mL of decane was measured inside a graduated cylinder and then poured inside the glass. The solution is then left to stir for 48 hours on a stirring plate.

3.2.4. Dynamic Light Scattering (DLS)

In order to measure the dispersion quality of the solutions before the ISR and Pendant Drop measurements, the DLS technique was applied. After sonicating the solution of the particles for 30 minutes, it is diluted to a new solution of 0.1 w% of particles and then placed in a cuvette. The cuvette is placed inside the equipment and the measurement begins. DLS results allows to analyze the particles sizes and their Polydispersity Index (PdI), used to estimate the average uniformity of a particle solution. If this value is over 0.3, the solution is too polydisperse and more sonicating is needed.

3.2.5. Interfacial Shear Rheometry (ISR)

Interfacial shear rheometry measurements were performed using a high-precision oscillatory stress-controlled rheometer (DHR-3 TA Instruments, Germany) with a double wall Du Noüy ring (20 mm ring diameter, 0.36 mm wire diameter) placed at the interface and shear in oscillating manner. Figure 11 shows a schematic overview of the IST operating. Time tests (constant angular frequency of 0.1 rad/s and constant torque of 0.01 μN.m) and frequency tests (angular frequency from 0.06 to 10 rad/s) were performed. The samples were repeated in triplicate showing similar plateau values.

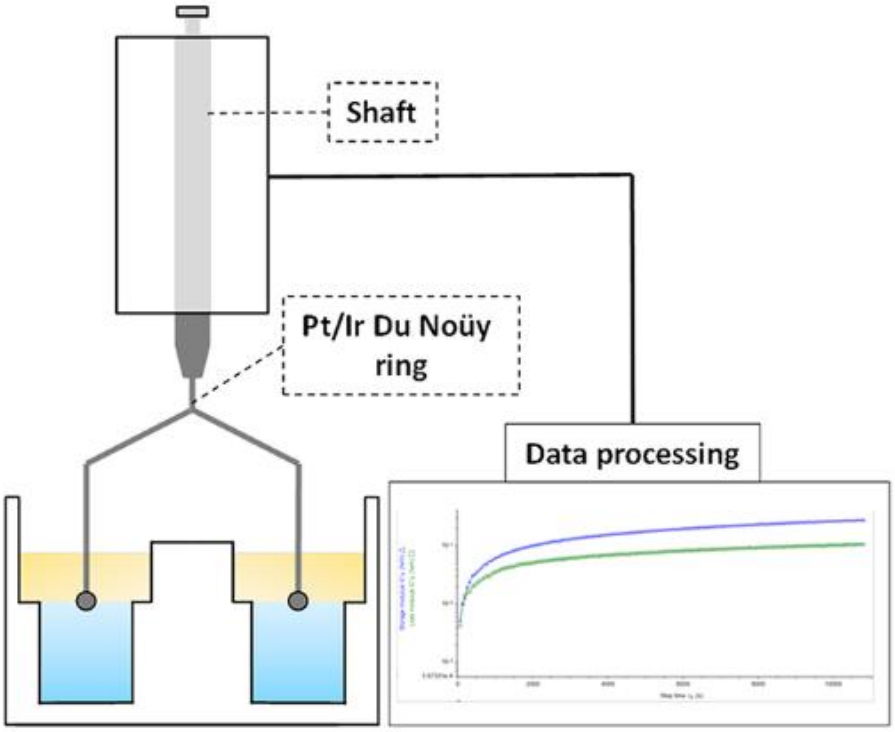

Figure 11: Schematic overview of the Interfacial Shear Rheometer.operating equipped with a Du Noüy ring. (SMITS et al., 2019)

The procedure was performed with both phases at 25°C. The first step in initiating the rheometer analysis was to place the particle solution in the ultrasonic bath for 30 minutes, ensuring a good dispersion of the particles. After the cleaning process for the ring and the block, the ring is positioned in the equipment and then, before every measurement, a calibration of the geometry is performed. Right before starting the measurements, the pH of the particle solutions is adjusted. For the measurements without particles on the aqueous phase, no sonication was needed.

Following the previous preparation, 5.8 mL of the aqueous phase is transferred carefully with the assistance of a pipet to the Delrin block. After that, the ring is placed submerged right below the surface of the water phase and then set to a fixed position. Following, the ring Is slightly moved, by placing it carefully at the interface. Subsequently, 3 mL of the oil phase was carefully placed on top of the aqueous phase very carefully without disturbing the interface. Lastly, a protection cover is placed around the equipment to avoid major external interface and the program is set to begging.

3.2.6. Pendant Drop Dilatational Interfacial Rheology

A schematic overview of the Pendant Drop measuring technique is showed in Figure 12. With the help of a glass pipet, approximately 1 mL of the water phase is poured inside a cuvette and then placed with the needle inside of it, in order to place the solution on the equipment. After that, the needle is cleaned twice with a clean wipe and them 900 µL of the oil phase (pure decane or 1mM SA) is poured into a cuvette and then placed on the equipment with the needle tip submerge on the oil phase. A pendant water phase drop of 5−10 µL is formed at the nozzle of the cannula (1.07 mm outer diameter), then IFT measurements was started, followed by frequency tests after 1 hour. All measurements were repeated three times, and the deviation between identical measurements was calculated.

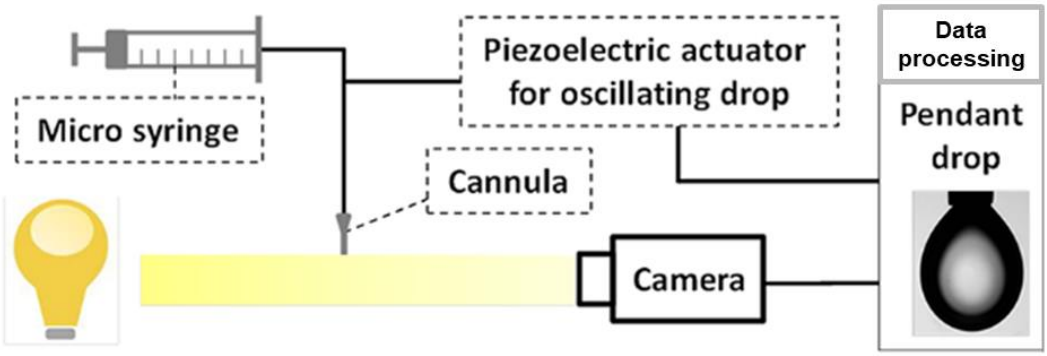

Figure 12: Schematic overview of the Pendant Drop dilatation interfacial theology technique operating. Adapted from (SMITS et al., 2019).

3.2.7. Sample preparation for Scanning Electron Microscopy (SEM)

Also as a qualitative analysis, SEM pictures of the monolayer were obtained in order to analyze how the particles are distributed at the interface. The samples were prepared using Langmuir−Blodgett-type transfers of interfacially adsorbed particles, Figure 13 shows a schematic illustration of the process.

For that, 30 mL of the aqueous phase is placed in a beaker, on a vibration-free table in a room with constant temperature at 20 °C. Then 12 mL of the oil phase is placed very carefully above the water phase, using a pipet and placing its tip slightly in the inside of the beaker, so that the liquid would flow easily to the interface. The oil phase

was composed of decane, stearic acid in a concentration of 1mM and 2 mL of tetraethyl orthosilicate (TEOS), this last chemical was used on the purpose of improving the film deposition at the crystalizing dishes. After setting the system, it is let sit for 24 hours to make sure the film is formed. After that time, the oil phase is carefully removed with the assistance of a pipet. Then, using a clean tweezer, the crystalizing dishes are placed carefully in the bottom of one side of the beaker, then it slid until the other side and is removed facing the front part upwards. With a wipe, the bottom part is carefully dried and the crystalizing dishes is placed on a holder. After that, the sample dries itself.

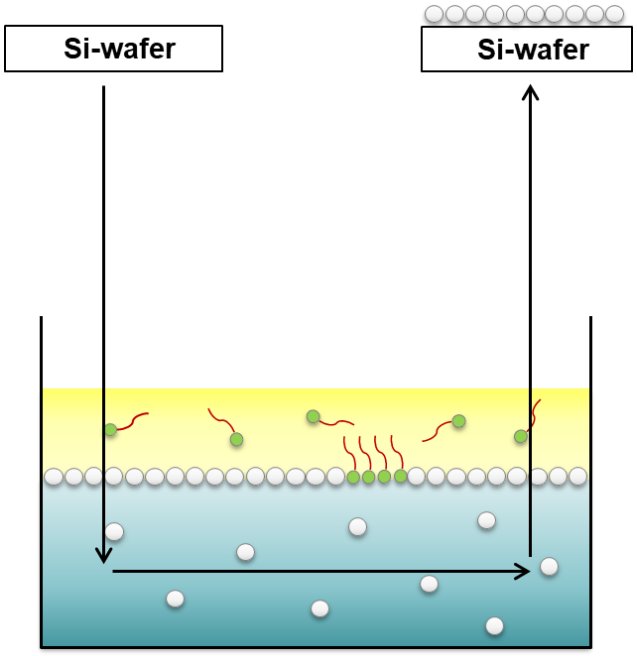

Figure 13: Schematic illustration of the Langmuir-Blodgett-type transfer of the particles film to the crystalizing dishes for SEM analysis.

4. RESULTS AND DISCUSSION

The system studied consists of the formation of a thin film formation of silica nanoparticles at the interface of a water-oil system with surfactants. As this work aims at packing of small particles in the interstitial gaps between the bigger ones, it is desirable for the particles to be able to rearrange themselves after getting to the interface. For that matter, the general design of the studied system is based on the interfacial adsorption of particles and surfactants of the same charge to avoid direct particle−surfactant interactions. Silica nanoparticles are naturally negatively charged so the surfactant chosen was stearic acid, which also is negatively charged (MAAS; OOI; FULLER, 2010; SMITS et al., 2019; YADAV; RAIZADAY, 2016). Studies were performed in a system with 1 w% silica nanoparticles at the water phase and 1mM stearic acid surfactants at the oil phase.

4.1. SCANNING ELECTRON MICROSCOPY (SEM)

In order to examine how the particles in our system would behave at the interface by a semi-quantitative assessment, SEM analysis of Langmuir-Blodgett-type transfers were performed.

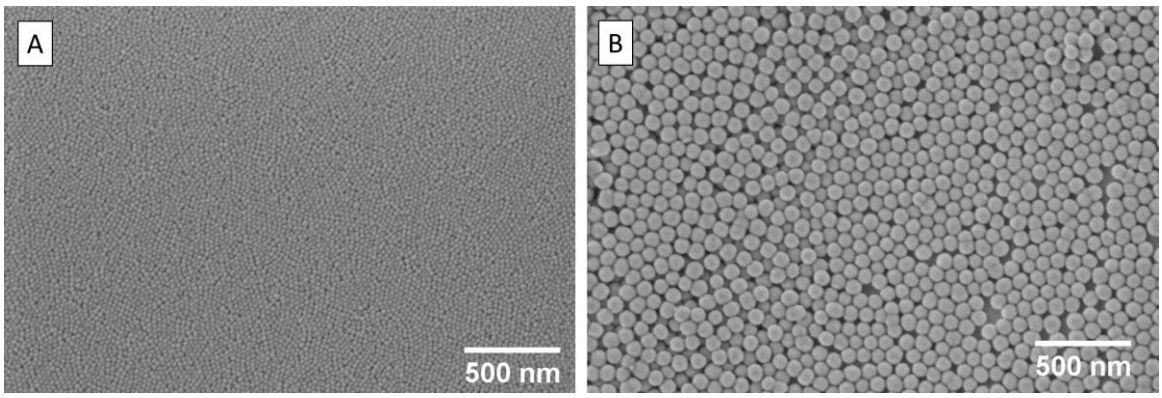

Figure 14: SEM images of particles transferred from the water-decane interface for two different sizes of silica nanoparticles in a system with (A) 25 nm and (B) 80 nm,, after 24 hours of equilibration.

At first, the particles were analyzed separately and a well packed thin film were observed for both of the particle sizes (Figure 14). In Figure 15 and Figure 16 the hexagonal packing of the particles is indicated with red contours. The packing of the particles shows to be mainly hexagonal, with a high order, but it is still possible to observe some defects, as larges holes between the particles. This could be due to irregular packing at the self-assembly or could have been induced in the preparation of the samples. What is also

possible to observe in this images is that, for the same area of film, there are more contact point for the smaller particles than for the bigger particles, what can relate to the results achieved in interfacial shear rheology, explained on topic 4.2.

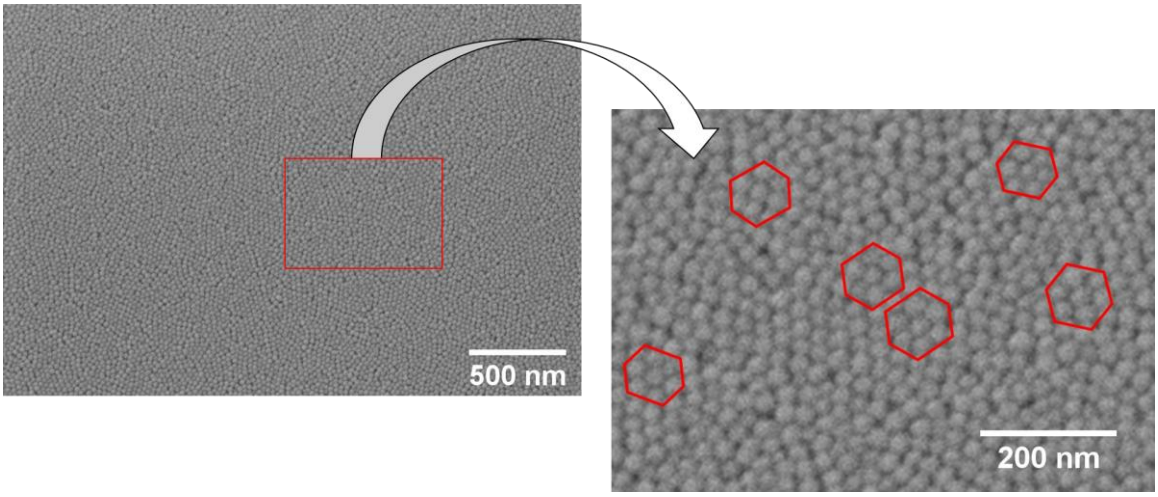

Figure 15: Close-up at the SEM image of the film created at the system with only 25 nm particles.

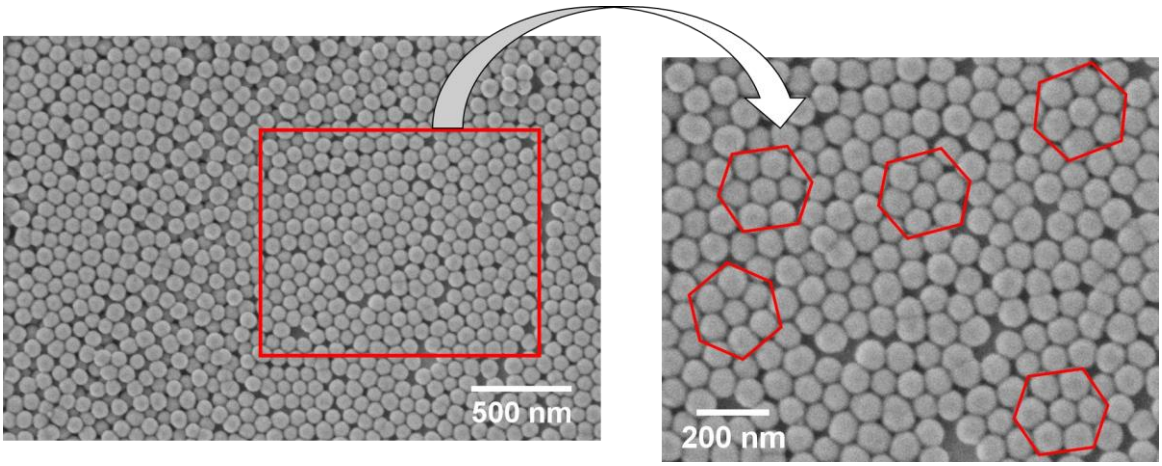

Figure 16: Close-up at the SEM image of the film created at the system with only 80 nm particles.

SEM images of the film created for the systems with mixed particles of different sizes (25 and 80 nm) is showed on Figure 17. The mixtures were prepared in different number ratios of large and small particles and are expressed by LS, were L indicates the portion of 80 nm particles (large) and S the portion of 25 nm particles (small). It is still possible to observe the formation of a well packed thin film for the mixtures, however, the packing behavior of the system was not in accord to what was expected. Figure 18 shows a close-up of the system with number ratio of LS_3, representative of the other mixtures. We can see here that the packing of the system does not follow a specific rule, but it is more randomly organized. It is possible to observe that at some points (indicated in red contours) the smaller particles surround the bigger ones, forming a denser layer, however, the bigger ones do not form a hexagonal assembly. On the other hand, at some regions it is possible to see that the

smaller particles agglomerate and form a hexagonal packing, not connected to the bigger ones, indicating strong connections between the particles of the same size. Figure 19 shows another behavior seen on this method and system, where the smaller and bigger particles segregate on the film, forming islands of only one size particles, generating big discontinuities on the film. These behaviors of packing create discontinuities, lowering the density of the film when compared to the film with particles of only one size.

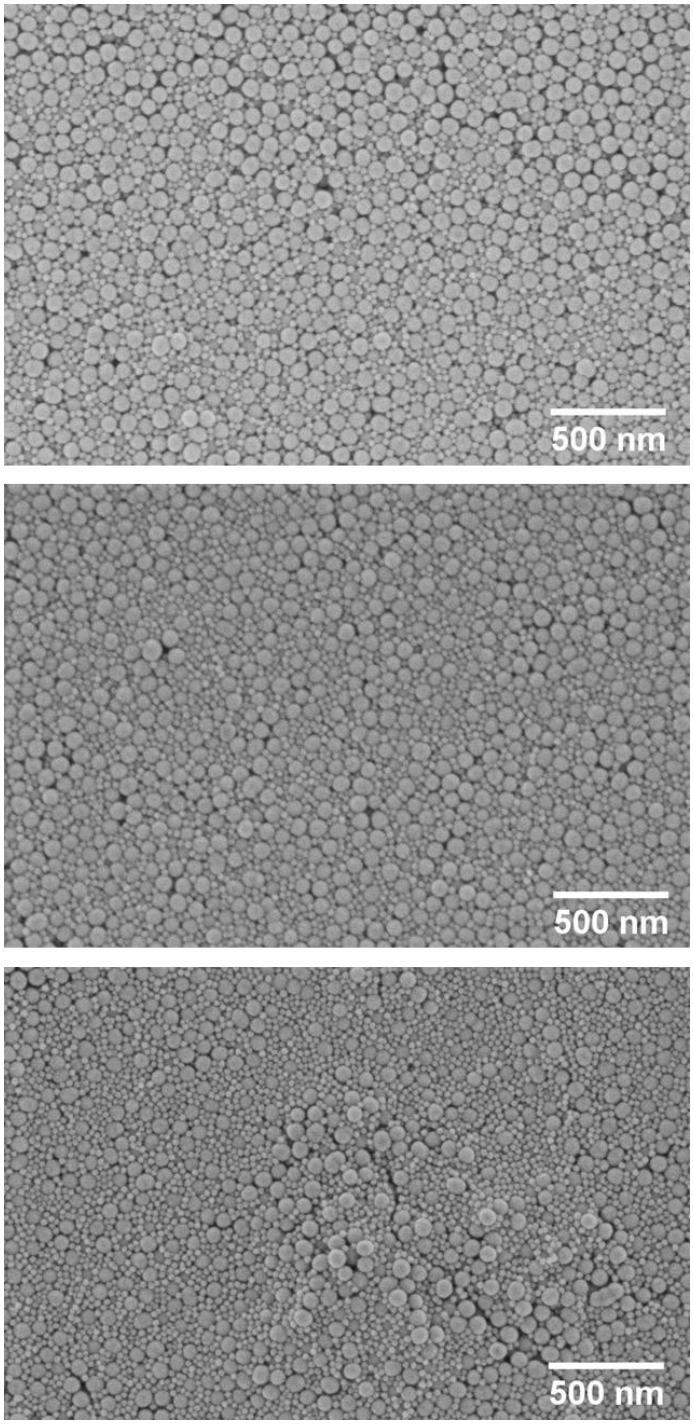

Figure 17: SEM images of particles transferred from the water-decane interface for different number ratio of mixtures made from 25 nm and 80 nm diameter-sized silica nanoparticles, after 24 hours of equilibration. (A) LS_2; (B) LS_3; (C) LS_6.

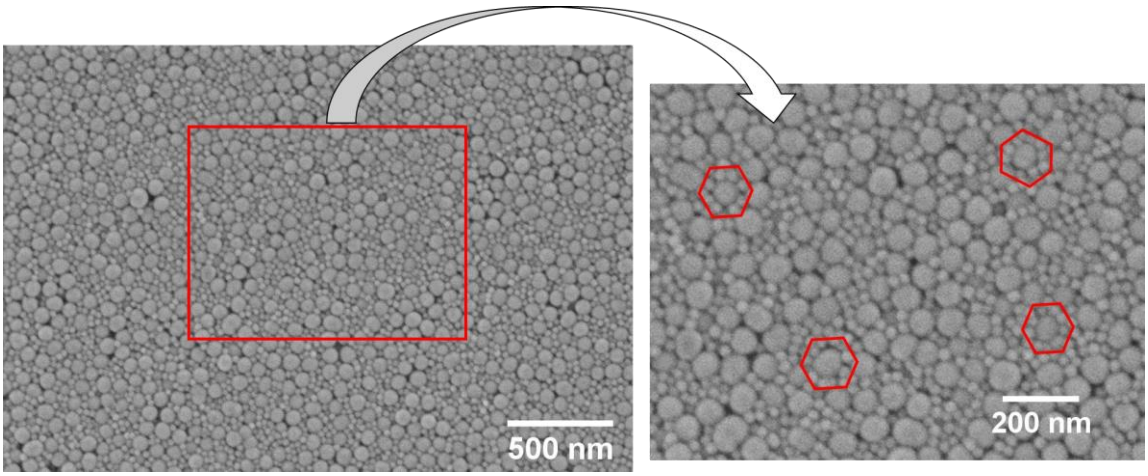

Figure 18: Close-up at the SEM image of the film created at the system for mixed particles with LS_3.

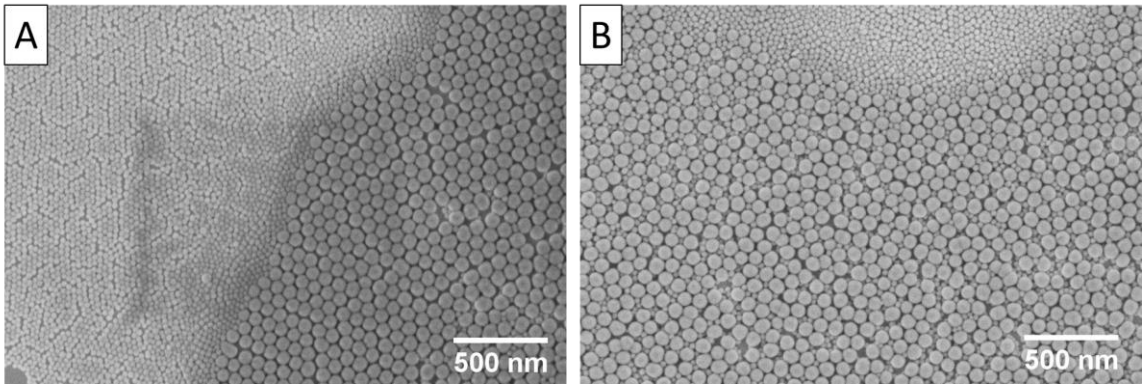

Figure 19: SEM images of particles transferred from the water-decane interface for mixtures with LS_3 of 25 nm and 80 nm diameter-sized silica nanoparticles, after 24 hours of equilibration showing phase segregation.

According to DAI et al., (2012), bigger particles have stronger pair-wise interactions between each-other over smaller ones, so they would preferably arrange in the hexagonal form and the smaller would rearrange between them, lowering the overall potential energy of the system. However, the overall strength of the interactions in the film will be higher with small nanoparticles due to the higher surface area.

On a self-assembly process, the particles use their thermal energy (kT) to equilibrate themselves, leading them to the interface and reaching the lower energy state or organization. However, there are discontinuities, like agglomeration and phase segregation, which can be considered minima (local or total minimum) when analyzing the energy landscape of the system. Even though the particle looks for the lower energy state, if they end up on one of the minima and their kT is not sufficient to overcome the energy of that state, they stay there and do not rearrange to a better one (LONGO; BLABER, 2016; SALADINO; ESTARELLAS; GERVASIO, 2017). A schematic illustration of a possible energy landscape for the system studied is shown in Figure 20, where the thermal energy of the particles is expressed by kT and the energy for the local minima as E_x.

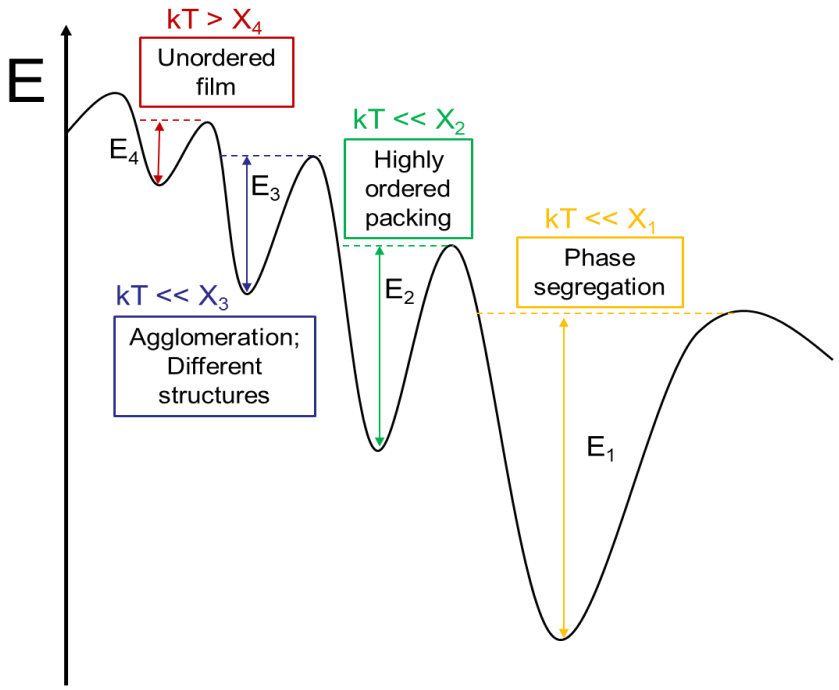

Figure 20: Schematic illustration of a possible energy landscape for the system studied.

Following this hypothesis for the system studied here, it is possible to conclude that the self-assembly process is not the ideal process of assembly to reach the well-structured film for the system studied.

In addition, when analyzing the simple theory of forces between the particles, the smaller ones, for a same area of the film, have more connection points when compared to the bigger ones, which indicates more Van der Waals bridges, indicating stronger interactions between them. Like discussed previously on this section, the mixed particles films showed that the smaller particles formed a hexagonal packing on some regions, however this behavior was not possible to observe for the bigger ones.

4.2. INTERFACIAL SHEAR RHEOLOGY

A more quantitative *in situ* analysis into the structural properties of the interface was achieved by investigating the different interfacial films with interfacial shear rheology. First we investigated separately how the particles and the surfactants would behave at the formation of the film, without the interaction between them (Figure 21). For that, the following systems were measured: no particles (pure water) and no surfactants (pure oil); no particles (water at pH 9.8) + 1mM SA; 25 nm silica nanoparticles at pH 9.8 + pure decane (no surfactants). No signal for the storage modulus (G′) or loss modulus (G’’) was observed.

This behavior, when it comes to the system with only particles without surfactants is due to insignificant interfacial population and lack of structural ordering. The surfactants by itself also failed to show the formation of a structured film. These results show space for improvement for the system by combining both materials.

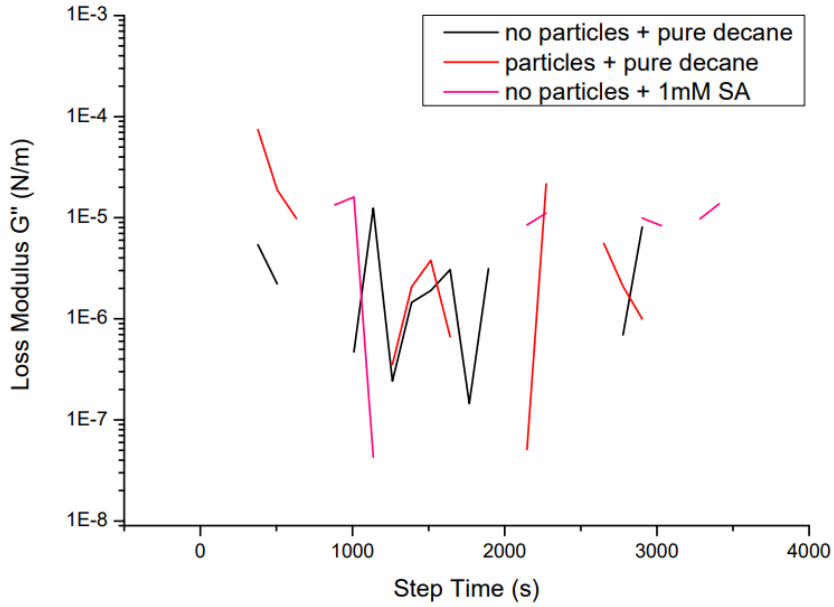

Figure 21: Loss Modulus (G'') from interfacial shear rheology for the reference systems.

Before mixing the two differently sized particles, they were investigated separately for the systems with 1 w% silica nanoparticles + 1mM SA surfactants. The formation of the film was investigated for a slightly acidic (pH 6) and basic (pH 9.8) systems, however, the film growth was only observed for the basic pH, as shows Figure 22. Stearic acid at the pH of 6 is almost neutral, so it will not be surface active, thus, when increasing the pH of the system to a very basic value, it will deprotonate the stearic acid at the interface, making it more surface active. As the surfactants will be strongly charged at a higher pH, their effect will be much more pronounced. In theory, the interactions of the two negatively charged species between each other are repulsive in nature, they assemble at the interface solely as a consequence to their phase separation, making uncertain if particle adsorption is even preferred over surfactant (CHEVALIER; BOLZINGER, 2013; XU et al., 2018). However, we have seen that the species separately do not form a structured film at the interface, restraining this phenomenon to the system with the interaction between them. As presented in the bibliographic review, negatively charged hydrophilic silica nanoparticles cannot adsorb at the interface, and in this case it depends on surfactants to make them surface active (CALZOLARI et al., 2012). In addition, the silica nanoparticles when reaching the interface will repeal each other, so not many particles will be able to adjust there, preventing the

formation of a dense film. However, when you have surfactants equally charged as the particles in the system, they will compete for the space at the interface, therefore, the surfactants will stay between the particles and for that, they can shield the electrostatic repulsion (SMITS et al., 2019).

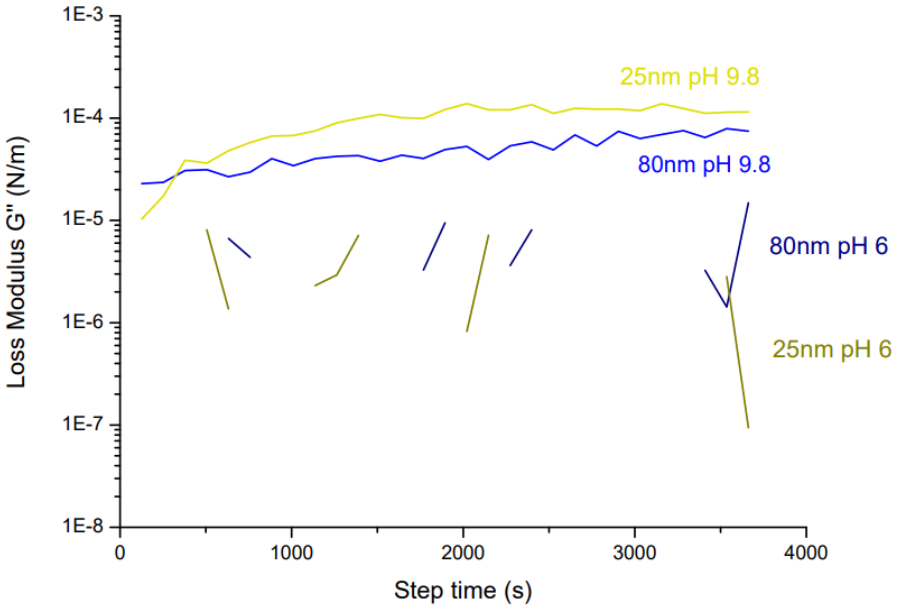

Figure 22: Loss Modulus (G") from interfacial shear rheology shows the time-dependent thin film formation of silica nanoparticles (1w%) and SA (1mM) at the decane/water interface, for 25 nm (yellow) and 80 nm (blue) particles, at the ph of 6 (darker color) and 9.8 (lighter color).

Figure 23 shows both Storage Modulus G' and Loss Modulus G'' for the time sweep tests performed. The film formation for the systems in the basic range is dominated by the viscous behavior, since G'' > G', therefore, the film behaves more liquid-like, showing some mobility, indicating that the film is able to equilibrate during the deformation (MEZGER, 2019). This mobility can be of the film itself moving around the interface or can also correlate to the dynamic mechanism of adsorption/desorption, proposed by SMITS et al., (2019), caused by competitive adsorption between the surfactants and the particles at the interface. The smaller particles (25 nm) showed a higher Moduli. When comparing the same area for a film with the smaller particles and the bigger particles, the smaller ones will show more cohesion points, which indicated more Van der Waal bridges. Therefore, the overall strength of the interactions on the film will be higher with small nanoparticles, as show the rheological results.

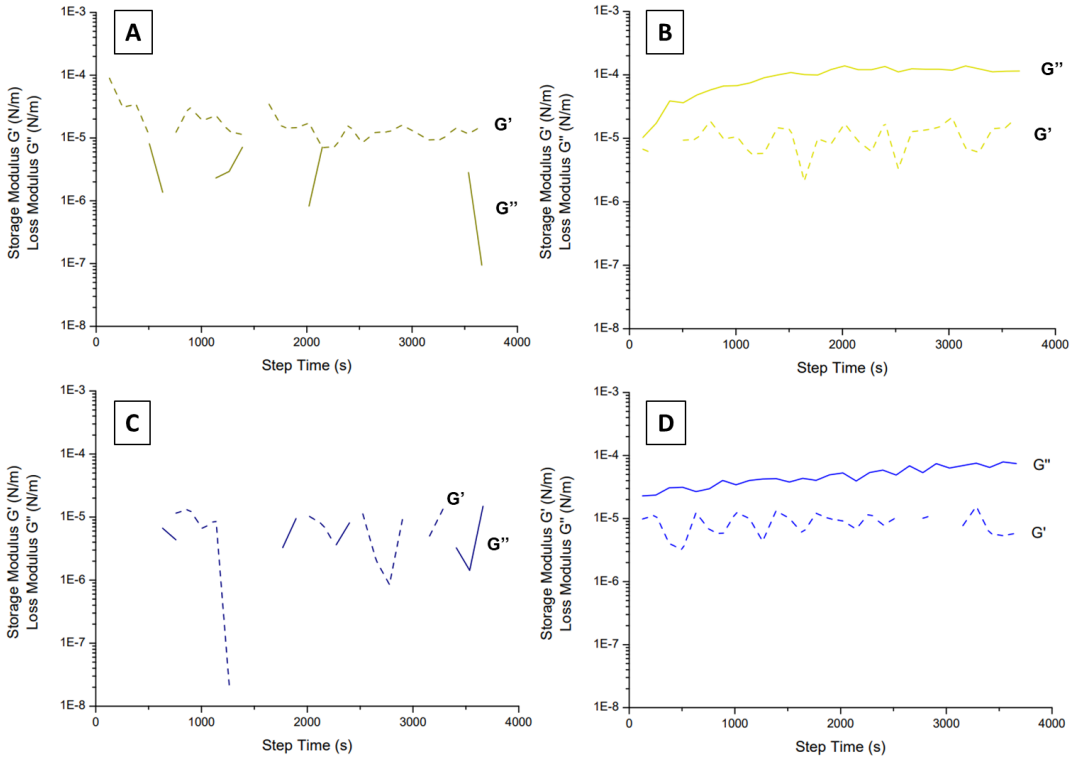

Figure 23: Loss Modulus (G") and Storage Modulus (G') from interfacial shear rheology shows the time-dependent thin film formation of silica nanoparticles (1w%) and SA (1mM) at the decane/water interface, for (A) 25 nm pH 6, (B) 25 nm pH 9.8, (C) 80 nm pH 6 and (D) 80 nm pH 9.8..

When analyzing the systems where the two different sized silica nanoparticles where combined (Figure 24), for all the four different number ratios, the film formation overall followed the same behavior as the systems with single-sized particles explained before. Here also we can see that the viscous behavior is predominant.

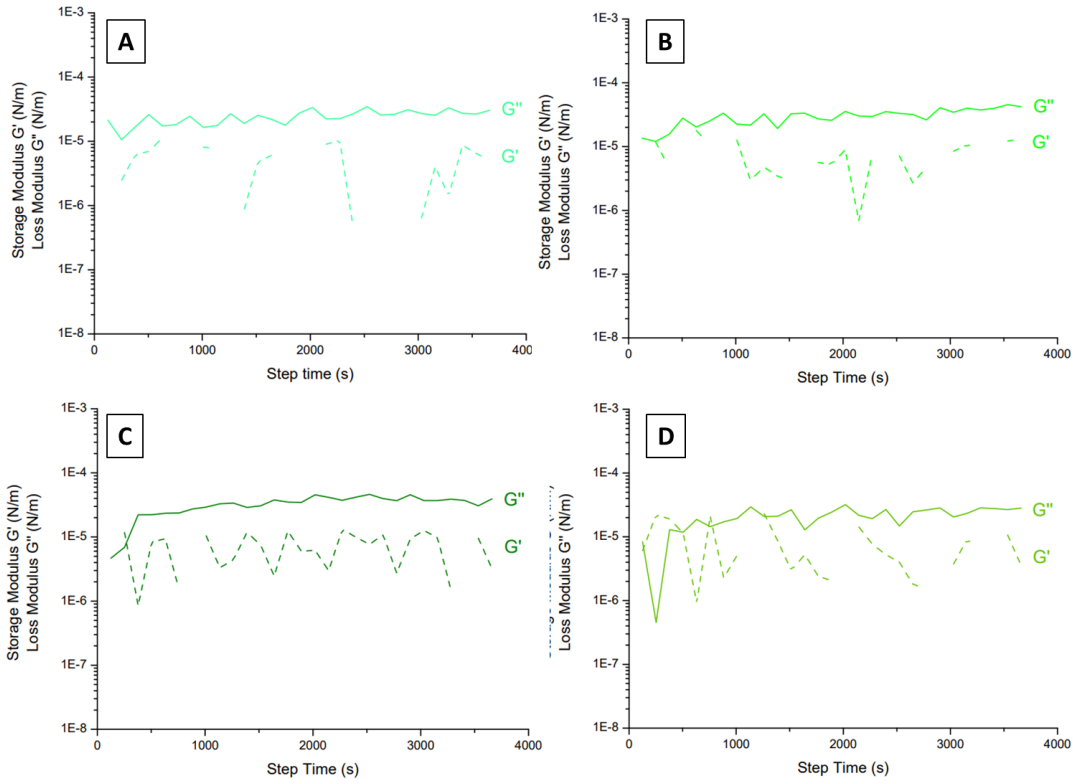

Figure 24: Loss Modulus G'' (line') and Storage Modulus G' (dots) from interfacial shear rheology shows the time-dependent thin film formation of different sized silica nanoparticles mixed at the pH of 9.8 (1w%) and SA (1mM) at the decane/water interface, for number ratio of (A) LS_2, (B) LS_3, (C) LS_4, (D) LS_6.

Reaching back to the main hypothesis in which this work is based, Figure 25 shows the time-dependent film formation, given by the loss modulus, for both single-sized and mixed systems. The aim of this work was to create a structure reinforcement on the film by improving its density when adjusting smaller particles between the hexagonal interstitial spaces between the bigger ones. However, as shown in the SEM results, the self-assembly technique for the used system and the chosen number and size ratios of particles were not favorable to reach this goal, instead of a higher order of packing expected for the mixed-particle films, it behaved more randomly than the films with one size particles. Since the particles when mixed where not so well packed, their density is lower and so, there are less contact points between the particles, hence, less forces between them, resulting in lower moduli. This fact is observable in the shear rheology results, as the moduli for the mixtures is slightly lower than for the single-sized systems.

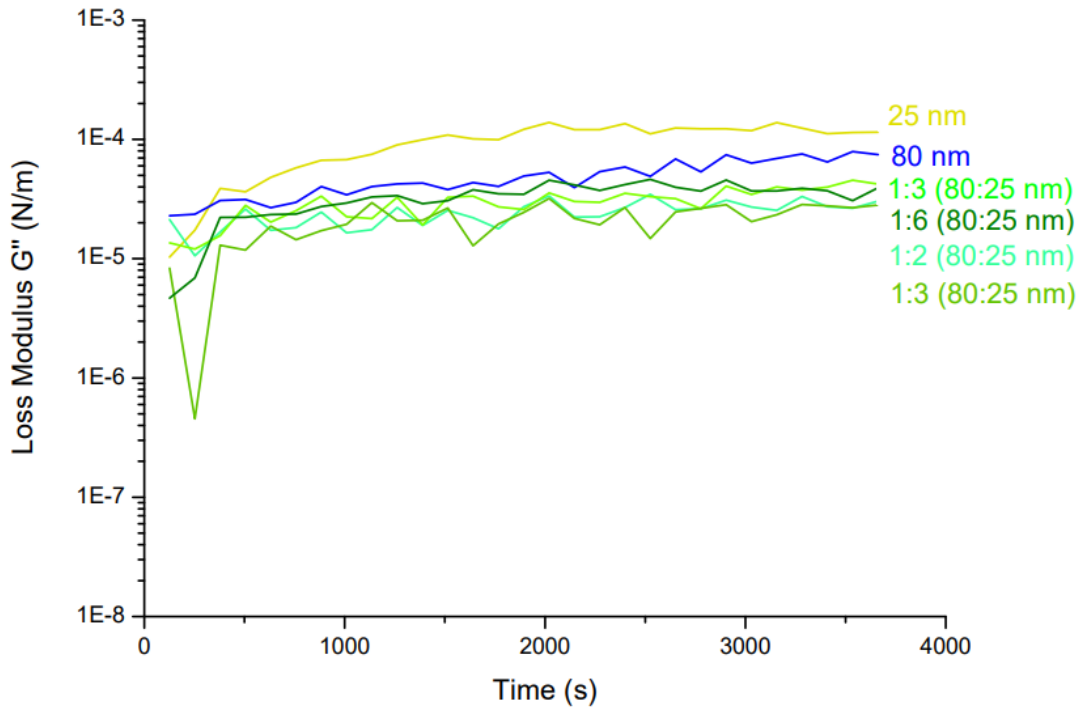

Figure 25: Loss Modulus G'' from interfacial shear rheology shows the time-dependent thin film formation of silica nanoparticles at the pH of 9.8 (1w%) and SA (1mM) at the decane/water interface, for 25 nm particles (yellow), 80 nm particles (blue) and different sized mixed particles (green) with number ratio of 1:2 (80:25 nm), 1:3(80:25 nm), 1:4(80:25 nm) and 1:6(80:25 nm).

To provide a more complete analysis of film formation, frequency sweeps were performed for the systems with 1 w% silica nanoparticles (25 nm, 80 nm and mixtures) at pH 9.8 + 1mM SA. Their behavior was predominantly similar, so only the results for the 25 nm particle system will be discussed. As presented in the Bibliographic Review, RENGGLI et al., (2020) introduced a method to calculate the inertia contribution present on the measurements for a DWR system. Figure 26 [A] shows the inertia plotted alongside the complex modulus dependent on the angular frequency. The method says that, in order for the inertia do not dominate the measurement, G* > Inertia Contribution. In our measurements, for the whole duration of the frequency test, the inertia did not dominate. On the other hand, when analyzing the phase angle for the system (Figure 26 [B]), it shows a linear behavior until the frequency of 1 rad/s, after that it starts to scatter, so it appears that something is not working well anymore for the film, even though the overall inertia as determined by Renngli's approach is not a problem.

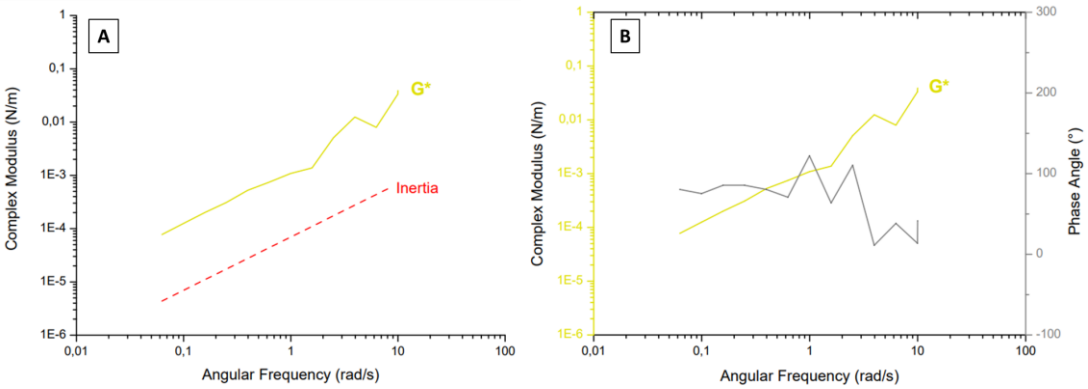

Figure 26: (A) Complex Modulus G and Phase Angle (°) from frequency sweep test of interfacial shear rheology of silica nanoparticles at the pH of 9.8 (1w%) and SA (1mM) at the decane/water interface for 25 nm particles. (B) Complex Modulus G* plotted with the Inertia Contribution calculation performed for the measurement.*

4.3. PENDANT DROP DILATATIONAL INTERFACIAL RHEOLOGY

With pendant drop interfacial dilatational rheology, interfacial tension (IFT) and moduli results were obtained as well. On Figure 27 we can observe that the systems without surfactants, either with (light and mid gray) or without (dark gray) particles, showed a steady IFT number of around 52.2 mN/m. Surfactants are very surface active, when adding it to a water-oil system, they will go to the interface and change the interfacial tension.

In the pendant drop system, when making the water phase droplet on the oil phase, the surfactants will rapidly go to the interface covering all of the surface and lowering the IFT considerably, however, they also leave the interface, leading then, to an increase at the IFT. This phenomenon is visible in Figure 27, the system with only water at pH 9.8 without surfactants is stable at the IFT value of 52.2 and then, when 1mM of SA surfactants is added to the system, the IFT rapidly decreases to a value around 12.5 mN/m and then goes up again, once the surfactants start leaving the interface, reaching a new plateau around 41 mN/m.

When measuring the relation of only particles with the interfacial tension, nothing is observed since they are not surface active and, therefore do not go to the interface (SMITS et al., 2019). However, when adding particles to the system with surfactants, they change the behavior of the system, since the particles will be now surface active and compete with the surfactants for a place at the interface, lowering the quantity of surfactants present there. The IFT values decrease similar to the systems without particles, however, these values do not go up as fast, since now there is less surfactants at the interface being able to leave it.

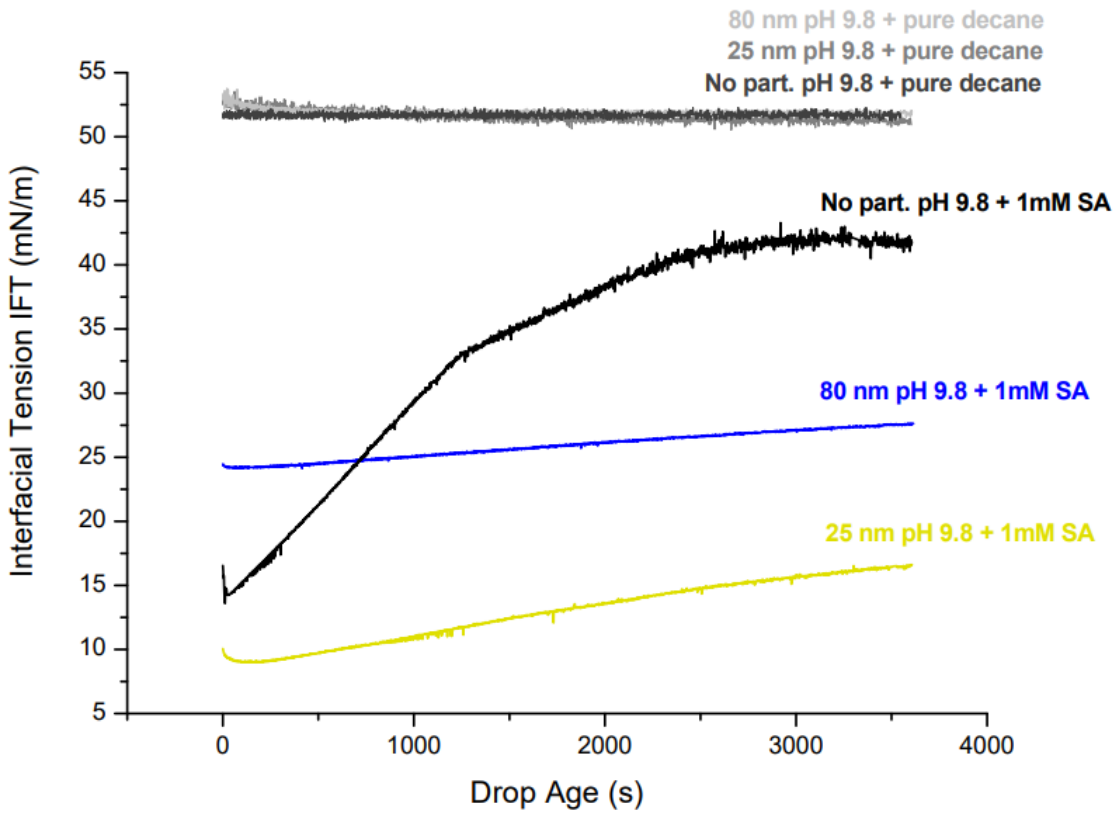

Figure 27: Interfacial tension (IFT) measurements. The light gray and middle gray lines shows a constant IFT for the system with particles in the absence of surfactants. The dark gray line shows a constant IFT for the system with no particles and no surfactants. The black line shows the rapidly decrease and then increase again of the system for stearic Acid without particles at the water phase at pH 9.8. The different colors represent different sized silica nanoparticles in the concentration of 1w% at the pH 9.8 on a system with 1mM SA on the oil phase.

When analyzing the particle systems with dual sizes, the smaller particles show a bigger difference in the IFT values (Δ IFT), indicating a more surface active system. When analyzing the rheological results shown in Figure 28, the smaller particles show a higher elasticity, going according to the IFT results. In the same area, more cohesive point between the particles will be present in the 25 nm particles films when comparing to the 80 nm particles films, resulting in greater forces and higher moduli.

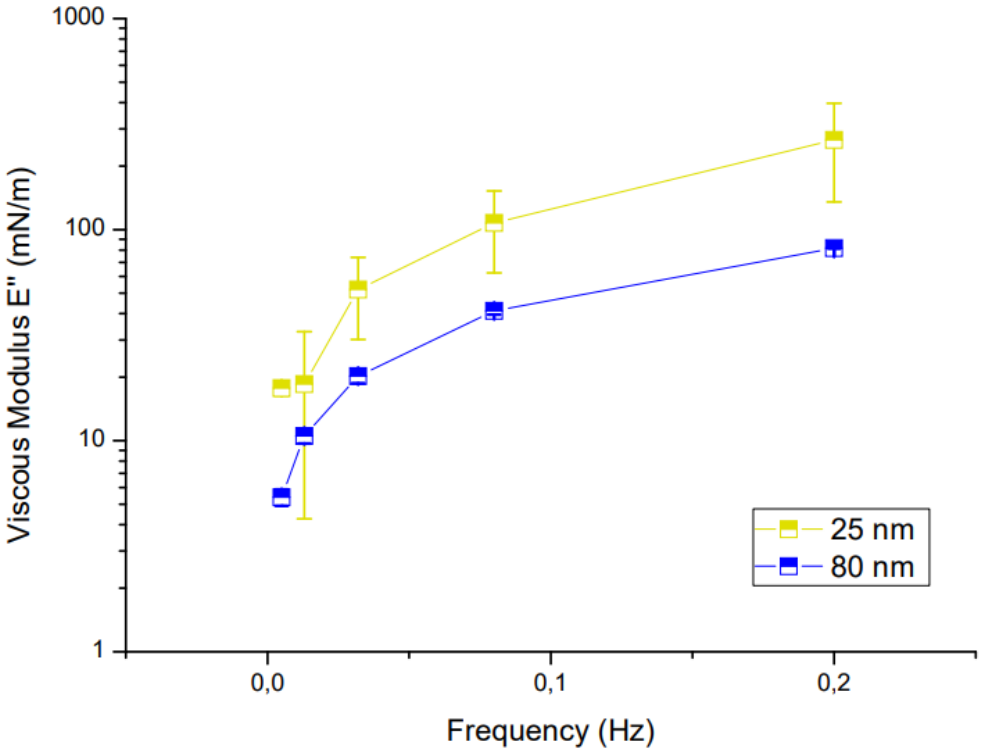

Figure 28: Frequency sweep results of dilatational interfacial rheology. In yellow is the Viscous Modulus E'' values (box) for the particles with 25 nm of diameter and in blue for the ones 80 nm of diameter. The standard deviation between the 3 measurements performed for each system is shown in error bars.

The mixed-sized-particles showed a IFT values in between the smaller and bigger particles, as presented in Figure 29. For the dilatation rheological results, shown in Figure 30 and Figure 31, the binary systems achieved a moduli in between the single systems. However, this difference is not so significant. Interfacial dilatational rheology does not evaluate the structure of the film, like shear rheology does, in this case, the binary systems results cannot be explained by the film ordering. In terms of cohesive points of interaction between the particles, the binary films will be between the two films with one size particles, therefore, this can be one explanation of why the dilatational rheological results behave as they do. Meanwhile, a much more detailed analysis of the surfactants behavior at the interface and the interactions is needed to have a more complex understanding.

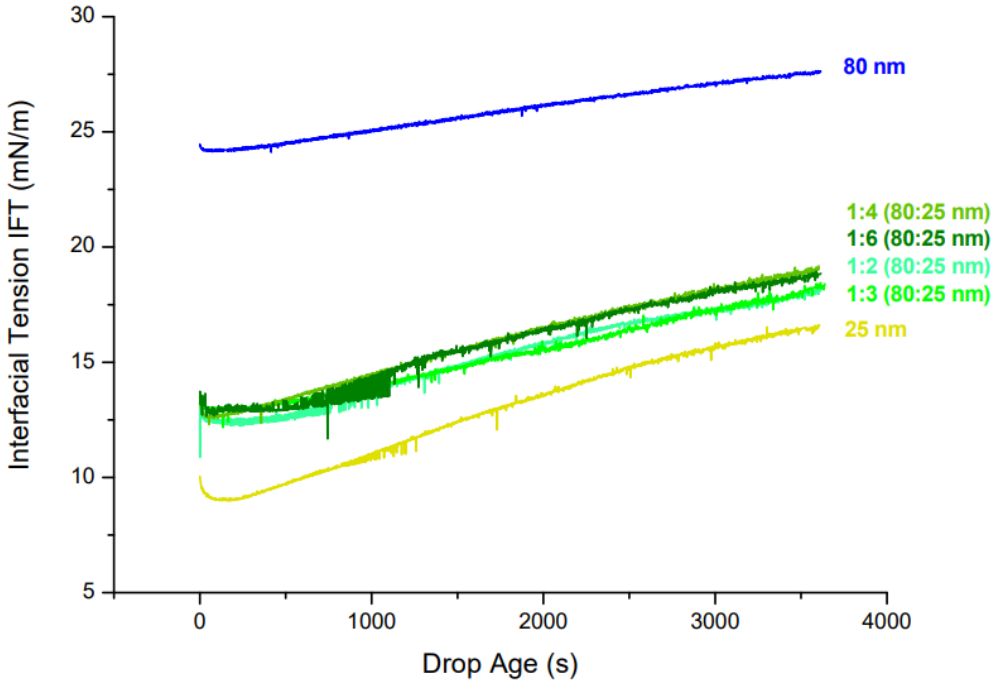

Figure 29: Interfacial tension (IFT) measurements for the systems with silica nanoparticles in the concentration of 1w% at the pH 9.8 + 1mM SA on the oil phase. The yellow line represents the results for the system with only 25 nm sized silica particles, the blue for only 80 nm sized particles and the different shades of green represents 4 different number ratios of mixed 25 nm and 80 nm particles.

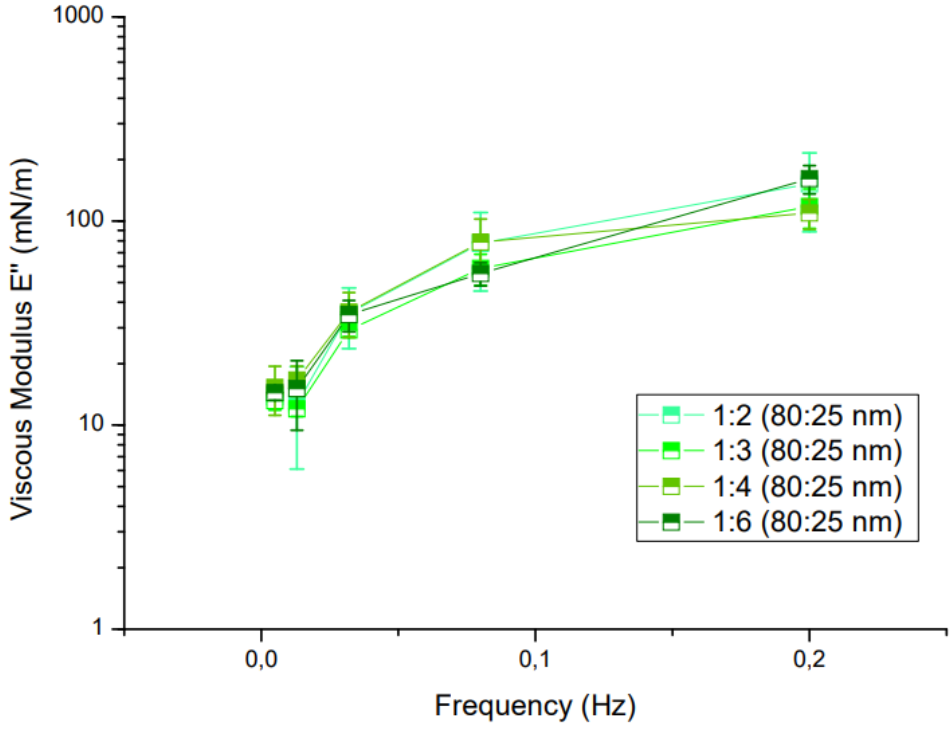

Figure 30: Frequency sweep results of dilatational interfacial rheology. Viscous Modulus E'' values (box) for the systems with mixed 25 nm and 80 nm sized silica particles, in different number ratios, are shown. The standard deviation between the 3 measurements performed for each system is shown in error bars.

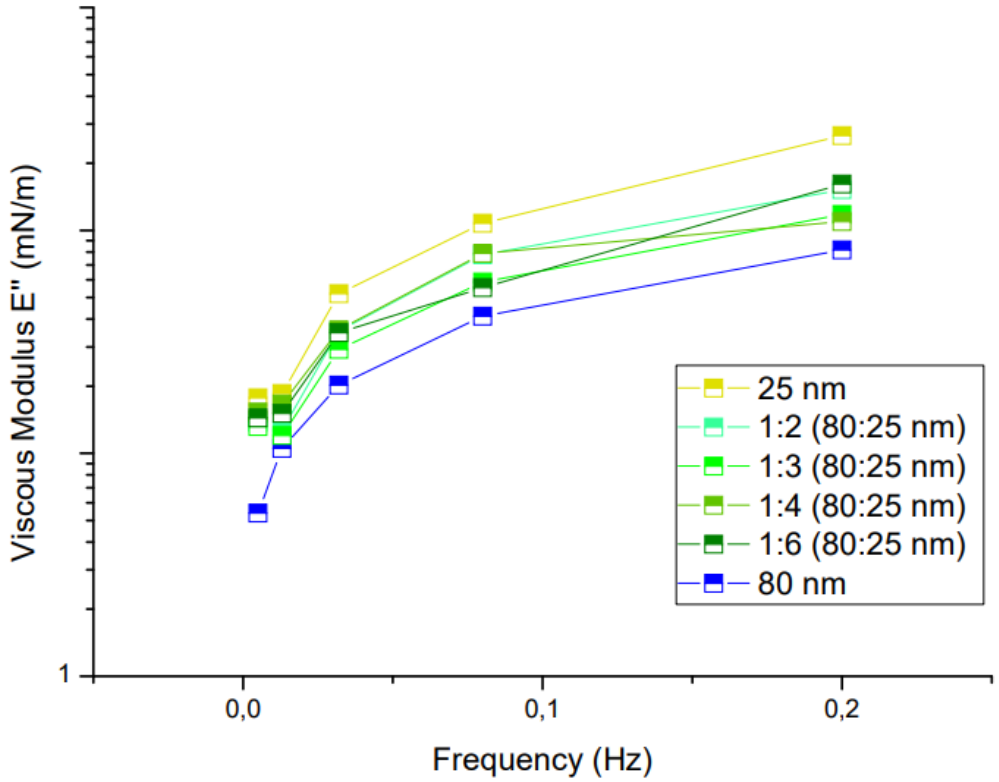

Figure 31: Frequency sweep results of dilatational interfacial rheology. In yellow is the Viscous Modulus E'' values (box) for the particles with 25 nm of diameter, in blue for the ones 80 nm of diameter and in green for the systems with mixed 25 nm and 80 nm particles, in different number ratios.

5. CONCLUSION

The aim of this work was to create a structure reinforcement on the film by improving its density when adjusting smaller particles between the hexagonal interstitial spaces between the bigger ones. The packing of a two-sizes mixed silica nanoparticles film in a water-oil interface in a system with surfactants equally charged as the particles was investigated. The reinforcement of the film structure was not validated. Through SEM analysis it was possible to observe that the smaller particles surround the bigger ones at some point, forming a dense layer, however, against our expectations, the bigger ones do not form a hexagonal assembly. At some regions is possible to see that the smaller particles agglomerate and form a hexagonal packing, not connected to bigger ones. Smaller and bigger particles also segregated on some part of the film, forming islands of only one size particles. These behaviors of packing create discontinuities, lowering the density of the film when compared to the film with particles of only one size and, therefore, their moduli. One hypothesis created based on the energy landscape was that, even if the particles look for the lower energy state, if they end up on one of the minima (discontinuities in the film structure) and their kT (thermal energy used to reach the lower energy state) is not sufficient to overcome the energy of that state, they stay there and do not rearrange to a lower state energy. Shear interfacial rheology results also verify what was seen in the SEM images. The smaller particles showed a higher moduli and, therefore, a more structured film. The system showed film formation at a basic pH of 9.8, which can be explained by deprotonation of the surfactants and, therefore, higher surface activity. The viscous behavior was predominant, so the film behaves more liquid-like, indicating that it has some mobility. We suspect that the same behavior observed by SMITS et al., (2019) of a adsorption/desorption mechanism between the surfactants and particles is occurring in our system as well. The self-assembly technique used for the system studied proved not to be the best approach to reach the goal of assembling a highly ordered structures with 25 nm and 80 nm mixed particles, since is possible to see that the assemble of the particles changed throughout the film.

OUTLOOK

As an outlook for further researches and projects is the modeling of the energy landscape for different type of particles, number ratios and size ratios, creating, therefore, a map that could find a system with very sharp local minimum and less minima of disorder. In that context, another suggestion is the use of different sizes of silica nanoparticles, that would provide a different value of size ratio of small and large particles, for the system studied could result in a better packing of the particles at the film. Another idea is to investigate the influence of different ranges of pH on the behavior of the stearic acid surfactants at the interface would provide a deeper understanding on the mechanisms that are happening there.

REFERENCES

[1] BARTLETT, P.; CAMPBELL, A. I. Three-dimensional binary superlattices of oppositely charged colloids. **Physical Review Letters**, v. 95, n. 12, p. 1–4, 2005.

[2] BINKS, B. P.; LUMSDON, S. O. Pickering emulsions stabilized by monodisperse latex particles: Effects of particle size. **Langmuir**, v. 17, n. 15, p. 4540–4547, 2001.

[3] BISHOP, K. J. M. et al. Nanoscale forces and their uses in self-assembly. **Small**, v. 5, n. 14, p. 1600–1630, 2009.

[4] BRESME, F.; OETTEL, M. Nanoparticles at fluid interfaces. 2007.

[5] BRÜGGER, G. et al. Controlling dispersion forces between small particles with artificially created random light fields. **Nature Communications**, v. 6, n. May, p. 1–7, 2015.

[6] CALZOLARI, D. C. E. et al. Nanoscale structure of surfactant-induced nanoparticle monolayers at the oil-water interface. **Soft Matter**, v. 8, n. 45, p. 11478–11483, 2012.

[7] CHEVALIER, Y.; BOLZINGER, M. A. Emulsions stabilized with solid nanoparticles: Pickering emulsions. **Colloids and Surfaces A: Physicochemical and Engineering Aspects**, v. 439, p. 23–34, 2013.

[8] DAI, Z. et al. Phase diagram, design of monolayer binary colloidal crystals, and their fabrication based on ethanol-assisted self-assembly at the air/water interface. **ACS Nano**, v. 6, n. 8, p. 6706–6716, 2012.

[9] DIBA, F. S. et al. Binary colloidal crystals (BCCs): Interactions, fabrication, and applications. **Advances in Colloid and Interface Science**, v. 261, n. August, p. 102–127, 2018.

[10] DU, K. et al. Adsorption energy of nano- and microparticles at liquid-liquid interfaces. **Langmuir**, v. 26, n. 15, p. 12518–12522, 2010.

[11] FENDLER, J. H. Nanoparticles at air/water interfaces. **Current Opinion in Colloid & Interface Science**, v. 1, n. 2, p. 202–207, 1996.

[12] HAMZA, R. A.; IORHEMEN, O. T.; TAY, J. H. Occurrence, impacts and removal of emerging substances of concern from wastewater. **Environmental Technology and Innovation**, v. 5, p. 161–175, 2016.

[13] KRALCHEVSKY, P. A. et al. Formation of two-dimensional colloid crystals in liquid films under the action of capillary forces. **Journal of Physics: Condensed Matter**, v. 6, n. 23A, 1994.

[14] KRALCHEVSKY, P. A.; NAGAYAMA, K. Capillary interactions between particles bound to interfaces, liquid films and biomembranes. **Advances in Colloid and Interface Science**, v. 85, n. 2, p. 145–192, 2000.

[15] LI, F.; JOSEPHSON, D. P.; STEIN, A. Colloidal assembly: The road from particles to colloidal molecules and crystals. **Angewandte Chemie - International Edition**, v. 50, n. 2, p. 360–388, 2011.

[16] LIN, Y. et al. Nanoparticle Assembly and Transport at Liquid-Liquid Interfaces. v. 299, n. Janurary, p. 226–229, 2003.

[17] LONGO, L. M.; BLABER, M. Proteins: Folding, Misfolding, Disordered Proteins, and Related Diseases. **Encyclopedia of Cell Biology**, v. 1, p. 108–114, 2016.

[18] MAAS, M.; OOI, C. C.; FULLER, G. G. Thin film formation of silica nanoparticle/lipid composite films at the fluid-fluid interface. **Langmuir**, v. 26, n. 23, p. 17867–17873, 2010.

[19] MEZGER, T. G. The Rheology Handbook. **The Rheology Handbook**, 2019.

[20] MISHRA, P. et al. **Application of Nanotechnology to Enhance the Nutrient Quality of Food Crops and Agricultural Production**. [s.l.] Elsevier Inc., 2018. v. 1

[21] MURRAY, B. S. Interfacial rheology of food emulsifiers and proteins. **Current Opinion in Colloid and Interface Science**, v. 7, n. 5–6, p. 426–431, 2002.

[22] NAKAMA, Y. **Surfactants**. [s.l.] Elsevier Inc., 2017.

[23] OH, J. R. et al. Fabrication of wafer-scale polystyrene photonic crystal multilayers via the layer-by-layer scooping transfer technique. **Journal of Materials Chemistry**, v. 21, n. 37, p. 14167–14172, 2011.

[24] OHARA, P. C. et al. = 0. 58,. v. 75, n. 19, p. 3466–3470, 1995.

[25] PAUNOV, V. N. et al. **Lateral Capillary Forces between Floating Submillimeter ParticlesJournal of Colloid And Interface Science**, 1993.

[26] POOLE, C. F. **High-Performance Precoated Stationary Phases**. [s.l.] Elsevier Inc., 2015.

[27] PRADO, A. G. S.; FARIA, E. A.; PADILHA, P. M. Aplicação e modificação química da sílica gel obtida de areia. **Quimica Nova**, v. 28, n. 3, p. 544–547, 2005.

[28] RENGGLI, D. et al. Operating windows for oscillatory interfacial shear rheology. **Journal of Rheology**, v. 64, n. 1, p. 141–160, 2020a.

[29] RENGGLI, D. et al. Operating windows for oscillatory interfacial shear rheology. **Journal of Rheology**, v. 64, n. 1, p. 141–160, 2020b.

[30] RICHARDS, T. Interfacial rheology: Principle, applications, and

instrumentation. **American Laboratory**, v. 33, n. 13, p. 38–39, 2001.

[31] SALADINO, G.; ESTARELLAS, C.; GERVASIO, F. L. **Recent Progress in Free Energy Methods**. Third Edit ed. [s.l.] Elsevier, 2017. v. 3–8

[32] SINGH, G. et al. Multicomponent colloidal crystals that are tunable over large areas. **Soft Matter**, v. 7, n. 7, p. 3290–3294, 2011.

[33] SMITS, J. et al. Reversible Adsorption of Nanoparticles at Surfactant-Laden Liquid-Liquid Interfaces. **Langmuir**, v. 35, n. 34, p. 11089–11098, 2019.

[34] TOMMASEO, G. et al. Hypersonic acoustic excitations in binary colloidal crystals: Big versus small hard sphere control. **Journal of Chemical Physics**, v. 126, n. 1, 2007.

[35] TSABET, È.; FRADETTE, L. Effect of the properties of oil, particles, and water on the production of Pickering emulsions. **Chemical Engineering Research and Design**, v. 97, n. 1, p. 9–17, 2015.

[36] VELIKOV, K. P. et al. Layer-by-layer growth of binary colloidal crystals. **Science**, v. 296, n. 5565, p. 106–109, 2002.

[37] VOGEL, N. et al. Wafer-scale fabrication of ordered binary colloidal monolayers with adjustable stoichiometries. **Advanced Functional Materials**, v. 21, n. 16, p. 3064–3073, 2011.

[38] WANG, P. Y. et al. Self-assembled binary colloidal crystal monolayers as cell culture substrates. **Journal of Materials Chemistry B**, v. 3, n. 12, p. 2545–2552, 2015.

[39] XU, M. et al. Novel Oil-in-Water Emulsions Stabilised by Ionic Surfactant and Similarly Charged Nanoparticles at Very Low Concentrations. **Angewandte Chemie - International Edition**, v. 57, n. 26, p. 7738–7742, 2018.

[40] YADAV, H. K. S.; RAIZADAY, A. **Inorganic nanobiomaterials for medical imaging**. [s.l.] Elsevier Inc., 2016.

[41] YAN, H. et al. New pickering emulsions stabilized by silica nanowires. **Colloids and Surfaces A: Physicochemical and Engineering Aspects**, v. 482, p. 639–646, 2015.